Algerian Democratic Republic and Populaire

Ministry of Higher Education

and scientific research

Echahid Hamma Lakhder University of El-Oued

Faculty of Technology

Thesis presented for obtaining the

ACADEMIC MASTERS

Domain : Science and Technology

Sector : Electrical Engineering

Specialty : Electrical Control

Theme

Comparative Study of MPPT Techniques for Photovoltaic System

Realised by:

Guerrah Oualid

Henka Oussama

Supervisor:

Dr.Gacem Abdelmalek

University year : 2023/2024

Dedication

I dedicate this modest work to:

my father, may God have mercy on him.

my dear mother and all my family.

all my professors.

all my friends, each by name.

Guerrah Oualid

Acknowledgments

First of all, I thank Almighty God for the successful completion of my master's thesis.

I would like to thank all the professors of the Electrical Engineering Department.

I would especially like to thank my thesis supervisor, **Dr. Gacem Abdelmalek**.

For welcoming us into his research team, his precious advice, his patience, his kindness, and his constant encouragement throughout this work.

Abstract

Solar radiation serves as the primary energy source for photovoltaic (PV) systems, which convert sunlight directly into electricity through the photovoltaic effect. This study explores the fundamental concepts of PV systems and solar energy generation, considering variations due to location and seasonality. DC-DC converters play a vital role by efficiently converting voltage levels for stable power delivery.

To maximize PV system efficiency, Maximum Power Point Tracking (MPPT) algorithms continuously optimize the operating point to extract maximum power from solar panels under varying conditions. Three widely used MPPT algorithms – Perturb and Observe (P&O), Incremental Conductance (INC), and Artificial Neural Network (ANN) – are evaluated and compared.

The P&O algorithm relies on perturbations and observations, INC uses incremental conductance, while ANN leverages artificial intelligence for precise maximum power point tracking. This comprehensive analysis highlights the strengths, weaknesses, and suitability of each algorithm, providing insights to improve the overall performance and energy yield of PV systems.

Keywords :

Photovoltaic systems (PV), Maximum Power Point Tracking (MPPT), Solar energy Artificial Neural Networks (ANN),Perturb and Observe (P&O), Incremental Conductance (INC).

الملخص :

تُعتبر الإشعاع الشمسي المصدر الرئيسي للطاقة بالنسبة لأنظمة الطاقة الكهروضوئية(PV) ، والتي تحول ضوء الشمس مباشرةً إلى كهرباء من خلال التأثير الكهروضوئي. تستكشف هذه الدراسة المفاهيم الأساسية لأنظمة الطاقة الكهروضوئية وتوليد الطاقة الشمسية، مع الأخذ بعين الاعتبار التغيرات الناجمة عن الموقع والموسمية. تلعب محولات التيار المستمر (DC-DC) دوراً حيوياً من خلال تحويل مستويات الجهد بكفاءة لتوفير إمداد طاقة مستقر.

لتحقيق أقصى كفاءة لأنظمة الطاقة الكهروضوئية، تعمل خوارزميات تتبع نقطة الطاقة القصوى (MPPT) على تحسين نقطة التشغيل باستمرار لاستخراج أقصى قدر من الطاقة من الألواح الشمسية في ظل ظروف متغيرة.

تتم تقييم ومقارنة ثلاث خوارزميات MPPT واسعة الاستخدام - خوارزمية الاضطراب والمراقبة(P&O) ، وخوارزمية التوصيل التفاضلي(INC) ، وشبكة الخوارزميات العصبية الإصطناعية(ANN).

تعتمد خوارزمية P&O على الاضطرابات والملاحظات، بينما تستخدم خوارزمية INC التوصيل التفاضلي، في حين تستفيد خوارزمية ANN من الذكاء الاصطناعي لتتبع نقطة الطاقة القصوى بدقة. تُلقي هذه التحليلات الشاملة الضوء على نقاط القوة والضعف وملاءمة كل خوارزمية، وتوفر رؤى لتحسين الأداء الإجمالي وعائد الطاقة لأنظمة الطاقة الكهروضوئية.

الكلمات المفتاحية:

أنظمة الخلايا الضوئية (PV) ، تتبع أقصى نقطة للقدرة(MPPT) ، الطاقة الشمسية,الشبكات العصبية الاصطناعية (ANN), خوارزمية الاضطراب والمراقبة(P&O),خوارزمية التوصيل التفاضلي(INC)

Contents

List of Figures

List of Tables

List of Acronyms and Abbreviations

List of Abbreviations	
PV	Photovoltaic
MPP	Maximum power point
MPPT	Maximum power point tracking
P&O	Perturb and observe
INC	Incremental Conductance
ANN	Artificial neural network
DC-DC	Continuous-continuous converter
KVL	Kirchhoff's Voltage Law
PWM	Pulse Width Modulation
LED	Light Emitting Diode
MOSFET	Metal Oxide Semiconductor Field Effect Transistor

List of Acronyms	
D	The duty cycle
T	The total time period (S)
CH	The chopper
$f_{switching}$	The switching frequency (kHz)
G	The conductance value (1000 W/m^2)
R_{opt}	The optimal value of the load resistance (Ω)
R_c	The load resistance (Ω)
V_{oc}	Open circuit voltage (V)
I_{oc}	Open circuit current (A)
Rs	Series resistance (Ω)

Rsh	Shunt resistance (Ω)
L	Inductance (mH)
C	Capacitance (µF)
I_{sc}	The short circuit current (A)
Pmax	The value of the maximum real power (W)
η	The energy efficiency of the solar cell (%)
$P\gamma$	The incident light power on the surface of the cell
V_L	The voltage across the inductor (V)
W_{on}	The energy input provided by the source to the inductor when CH is on
W_{off}	The energy that the inductor releases to the load when CH is off

General Introduction

General Introduction

The world population is increasing rapidly, and energy consumption is rising. Consequently, greater electricity production is necessary to meet human needs, leading to an increase in the amount of resources required to produce it. However, the resources that have been primarily used so far, fossil fuels, are finite resources. Therefore, it is necessary to explore energy sources that are not depleted.

Solar energy certainly represents the most elegant renewable energy source. In addition to being silent, it integrates perfectly into buildings (facades, roofs, etc.), and because it does not include moving mechanical parts, it does not require special maintenance and remains reliable for a long time. This is why it has become a reference in space applications and in isolated sites. It is becoming a reliable option for small and medium energy consumption applications, especially since solar panels have become cheaper for better efficiency[1].

In this work, we study the improvement of efficiency and performance of photovoltaic solar energy production systems using a maximum power point tracking (MPPT) controller with changes in ambient weather conditions such as solar radiation and temperature. In this context, the work aims to simulate a photovoltaic energy production system consisting of a solar panel, and a DC/DC boost converter.

Chapter I

Solar Radiation

And

Photovoltaic Energy

I.1. Introduction :

Solar radiation, the most abundant energy resource on Earth, is the primary source of energy for photovoltaic (PV) systems. Photovoltaic energy, often referred to as solar energy, is harnessed through the use of photovoltaic cells, which convert sunlight directly into electricity.

In this chapter, we will discuss general information about solar energy. We will describe the basic concepts of photovoltaic systems and electricity production through the photovoltaic effect. We will explain how solar energy varies depending on location and season.

I.2. Solar Radiation :

Solar radiation refers to the entirety of the radiations emitted by the Sun. In addition to cosmic rays, particles characterized by extremely high speed and energy, the Sun emits electromagnetic waves that extend from the radio wave spectrum to gamma rays, passing through visible light.

The emission of electromagnetic waves by the Sun is accurately modelled by a black body at 5800 Kelvin, as described by Planck's law. The emission peak is in the yellow spectrum (λ=570 nm), with radiation distribution roughly evenly split between visible light and infrared, and 1% in ultraviolet. Upon reaching sea level, after traversing the entire Earth's atmosphere, solar radiation undergoes several "filtering" processes. Notably observable in the spectrum are the ozone absorption bands (known to absorb a significant portion of ultraviolet radiation), oxygen, carbon dioxide, and water [2] .

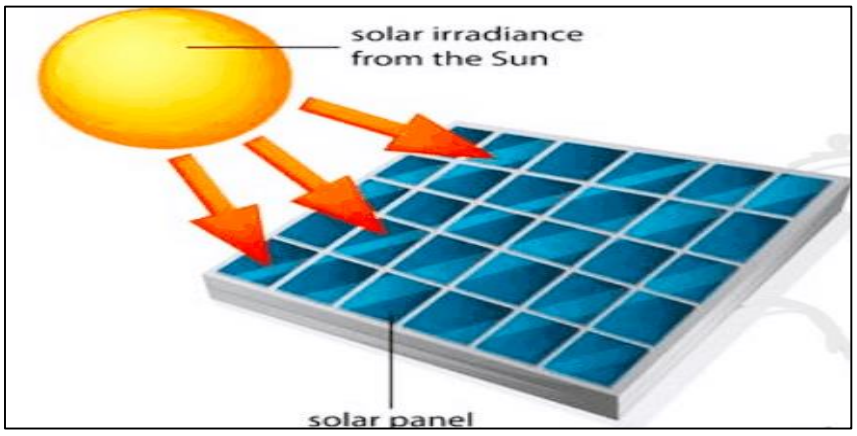

Figure (I.1): Representation of Solar Radiation

I.2.1. Radiation Spectrum:

The concept of solar energy may seem abstract, but in reality, it's what we have always known as heat and light from the Sun The invention of photovoltaic cells last century gave us the possibility of powering our civilization with solar energy. With photovoltaic solar panels, light energy is converted into a flow of electricity.

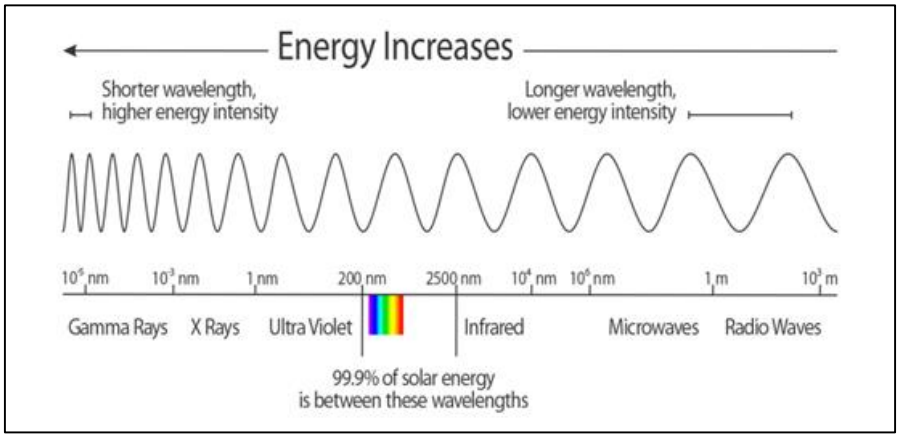

Figure (I.2): Solar Radiation Spectrum

While the electromagnetic spectrum is wide and vast, 99.8% of the Sun's radiant energy is emitted in a very narrow bandwidth from 20 to 2500 nanometers.

Only a small fraction of solar radiation reaches the Earth's surface, including radio waves with a wavelength of a few decameters to the softest ultraviolet rays, while the rest is either reflected or absorbed by the atmosphere and ionosphere [2].

Figure (I.3) illustrates the solar radiation spectrum. The composition of solar energy is approximately 5% ultraviolet light; 42% visible light and 53% near infra-red radiation.

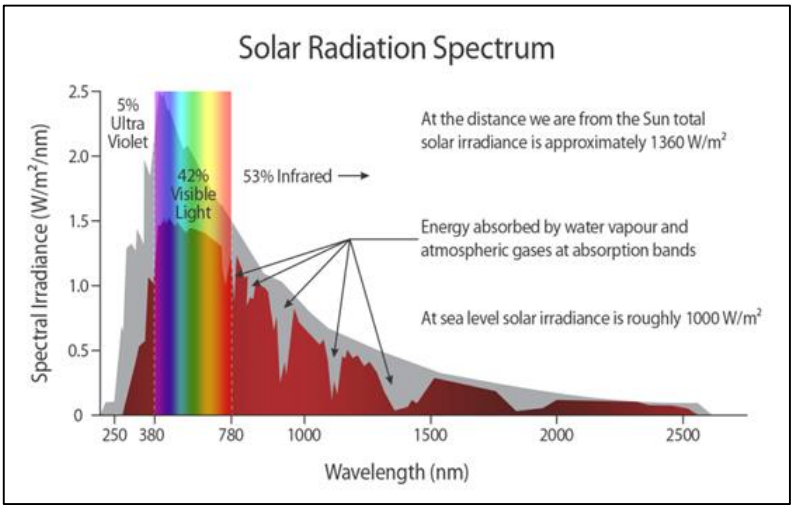

Figure (I.3): Representation of Solar Radiation Spectrum

I.3. Conversion of Solar Radiation by PV Effect :

A PV cell consists of two layers of silicon; these two layers are doped to be polarized. To make one of the layers positive ("P layer"), a certain number of boron atoms are incorporated, and to make the other layer negative ("N layer"), a certain number of phosphorus atoms are incorporated. This creates a potential barrier. When a photon with sufficient energy is absorbed by this semiconductor, it breaks a valence bond and releases an electron, creating a positive "hole". This is what is called the photovoltaic effect: it is the potential difference between these two layers. By connecting the two layers, there is a movement of electrons from one layer to the other, thus creating an electric current [1].

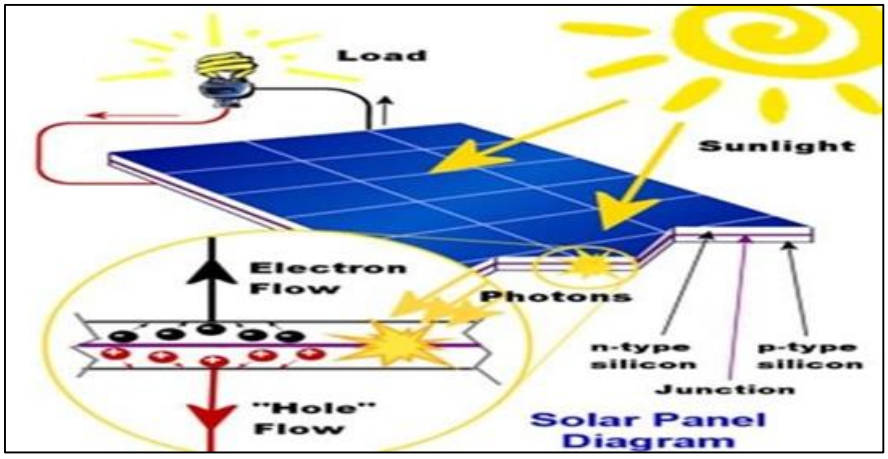

Figure (Ⅰ.4): Solar Radiation Conversion by PV Effect

I.4. Photovoltaic Generator :

The photovoltaic sensor is characterized by its electrical properties, particularly the relationship between current and voltage (I=f(V)), as illustrated in Figure (I.5).

This modelling is commonly used to estimate the sensor output (voltage, current) based on two input variables: temperature and the illumination received by the sensor.

The current produced by the photovoltaic module at a given voltage depends exclusively on the illumination and the temperature of the cell. With temperature and illumination constant, the efficiency of a solar cell is influenced by the load present in the electrical circuit. In an open circuit configuration ($R_c = \infty$, $I = 0$, $V = V_{oc}$) or a short circuit ($R_c = 0$, $I = I_{sc}$, $V = 0$), no energy is transmitted outside. Between these two extremes, an optimal value R_{opt} of the load resistance Rc exists, for which the power

($P=V_{max} \times I_{max}$) provided by the solar cell to the load resistance is maximal, thus reaching P_{max} [3].

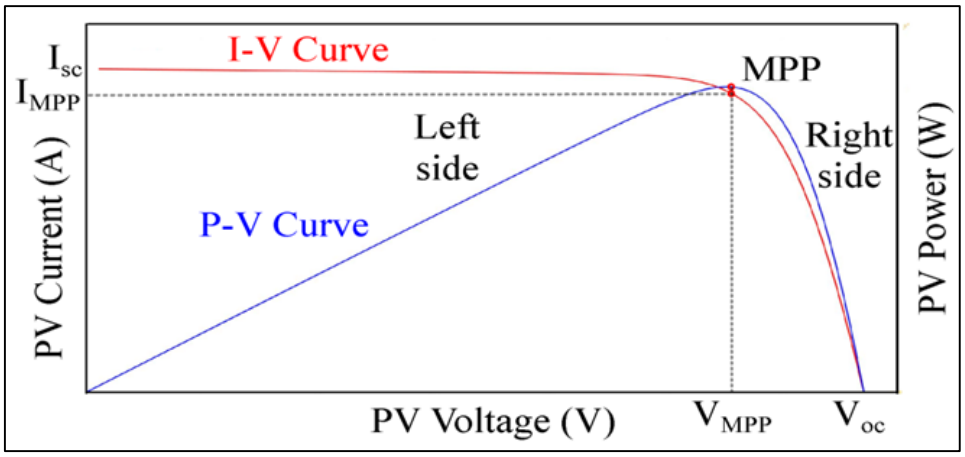

Figure (I.5): Typical Characteristics of a PV Generator

The energy efficiency of the solar cell is defined as $\eta=P/P\gamma$, where $P\gamma$ is the incident light power on the surface of the cell. For the optimal value R_{opt} of the load resistance R_c, the efficiency of the solar cell is maximum, and $\eta_{max}=P_{max}/P\gamma$. The value of R_{opt} is not a characteristic constant for a given cell, but depends on the spectrum of the incident radiation and the junction temperature. In fact, the efficiency decreases as the temperature increases, which sometimes leads to the construction of hybrid sensors resulting from the combination of a thermal sensor and a solar cell. These sensors allow the simultaneous production of hot water and increase the photovoltaic efficiency by cooling the cell.

The power provided by the solar cell ($P=I\times V$) and its efficiency depend on the material used and the manufacturing technology (amorphous silicon, polycrystalline silicon, monocrystalline silicon), the junction geometry (layer thickness, multilayers, etc.), and external parameters (temperature, spectrum and power of the incident radiation, external electrical circuit connected to the cell, etc.).

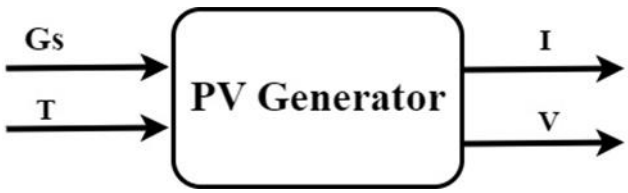

Figure (I.6): Block Diagram of a PV Generator

I.4.1. Photovoltaic Cell :

Photovoltaic modules consist of an arrangement of interconnected solar cells. These cells are embedded in resin and encapsulated between two tempered glass panes (double-glass modules) or between a glass pane and a Tedlar sheet (glass/Tedlar module). Typically, this assembly is inserted into an anodized aluminium frame, although frameless modules are available for building integration applications, using aluminium profiles on facades or roofs. The power that a module can provide depends on its surface area and the incident solar irradiation, expressed in peak watts (W_p), and represents the maximum power of the module for a reference maximum solar irradiation (1000 W/m²).

The voltage delivered by a module depends on the number of cells connected in series. For low-power modules (< 75 W_p), the operating voltage is generally between 12 and 15 volts. Higher power modules are obtained by increasing the number of cells in series, which results in an "increase in voltage," and by increasing the number of cell branches in parallel, which causes an "increase in current value." The operating voltage can then be 24 volts or more, depending on the system configuration to be powered. The surface area of the modules varies among manufacturers, typically between 0.5 and 1 square meter; it can reach 3 square meters for special productions and large orders. Several interconnected modules form a panel, and several interconnected panels make up a photovoltaic array. Assembling modules in series and/or in parallel allows generating different voltages and powers [1].

I.4.2. Modelling of a PV Cell :

The operation of a photovoltaic module is described by the "standard" one-diode model, established by Shockley for a single photovoltaic cell, and then generalized to a photovoltaic module by considering it as a set of identical cells connected in series or parallel.

In the literature, a photovoltaic cell is often described as an electrical current generator whose behaviour is equivalent to a current source shunted by a diode. To account for physical phenomena at the cell level, the model is supplemented by two series resistances R_s and R_{sh}, as illustrated in the equivalent circuit diagram in Figure (I.7).

The series resistance represents the internal resistance of the cell and depends mainly on the resistance of the semiconductor used, the contact resistance of the collecting grids, and the resistivity of these grids. The shunt resistance is due to leakage current at the junction and depends on how it was made.

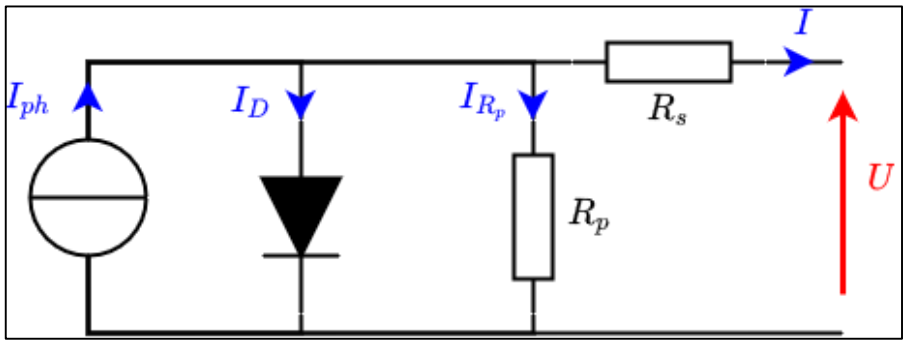

Figure (I.7): Equivalent Circuit of a PV Cell

I.4.3. Types of Photovoltaic Cells :

Photovoltaic solar panels are made up of photovoltaic cells and vary according to type:

1. Monocrystalline Cells : Monocrystalline silicon results from the cooling of molten silicon. Once solidified, it transforms into a uniform crystal that is cut into thin slices to form the photovoltaic cell. The colour of this material is blue, without any trace of crystals or other impurities.

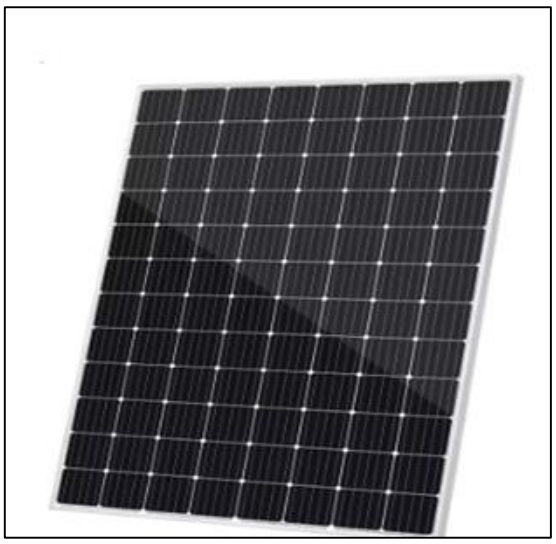

Figure (I.8): Monocrystalline Cells

2. Polycrystalline Cells : Polycrystalline silicon is obtained by melting silicon in a square and elongated metal mold, called an ingot. The color of this type of cell is blue and speckled with patterns left by the crystals. This characteristic allows us to easily recognize this photovoltaic cell.

Figure (I.9): Polycrystalline Cells

3. Hydrogenated Amorphous Cells : Amorphous silicon is obtained from silicon gas. This gas is vaporized onto a support, either glass, flexible plastic, or metal, using a vacuum deposition process. These PV cells are dark gray.

Figure (I.10): Hydrogenated Amorphous Cells

I.5. The Impact of Solar Radiation on Solar Panel :

Figure (I.11) show the influence of radiation on the I=f(V) and P=f(V) characteristics at a constant temperature. We maintained a constant temperature (25°C) at different radiation levels (200 ,400 ,600 ,800 ,1000 W /m²).

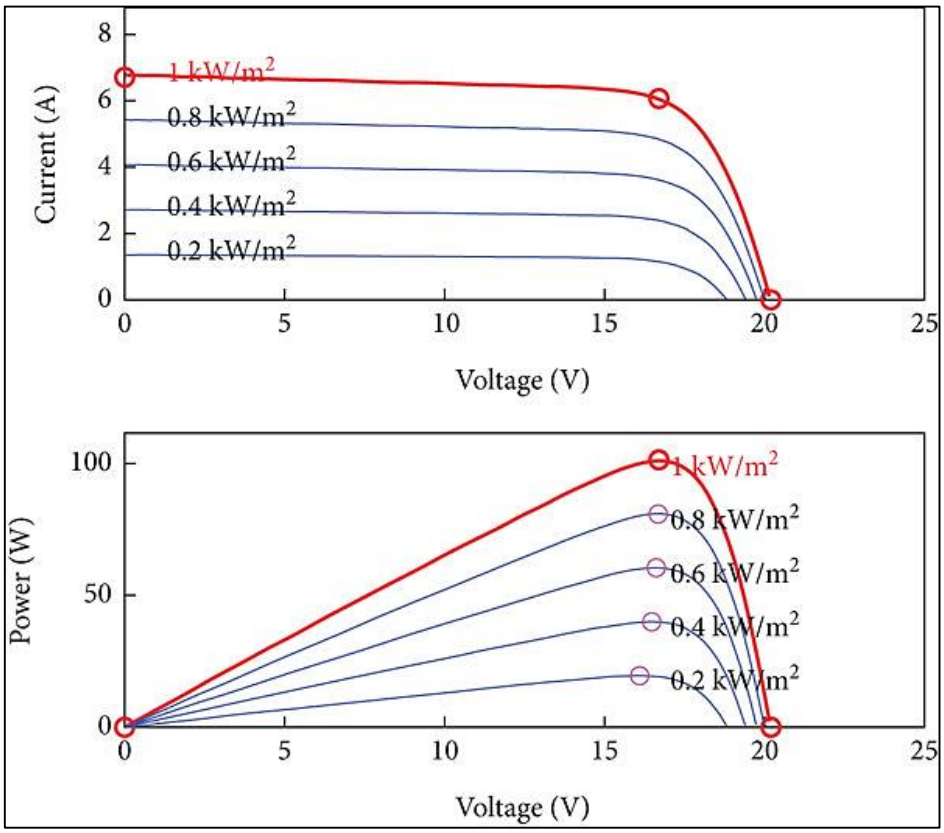

Figure (I.11): The Impact of Solar Radiation on Solar Panel

I.6. The Impact of Temperature on Solar Panel :

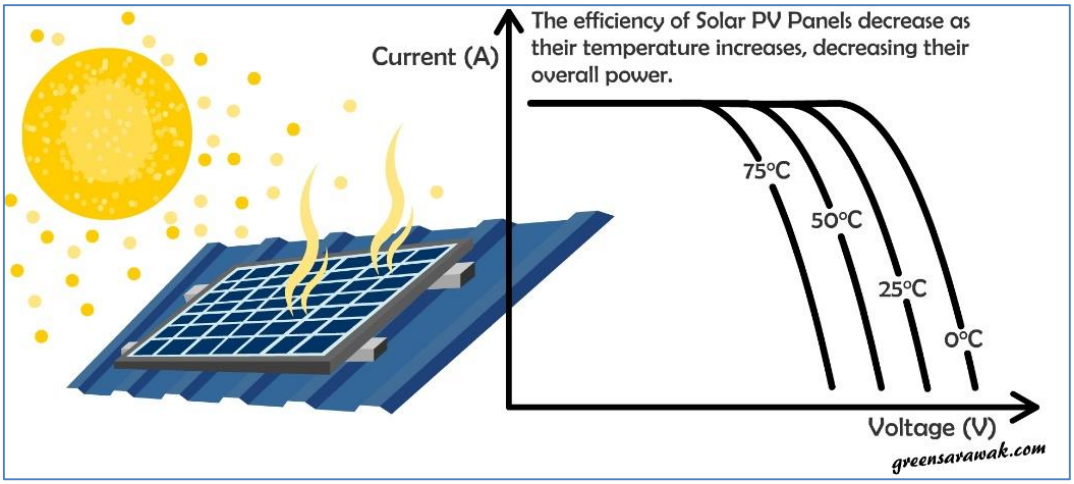

Figure (I.12): The Impact of Temperature on Solar Panel

Temperature has a significant impact on the performance of solar panels. Here's how:

- **Reduction in Efficiency :** As the temperature of solar panels increases, their efficiency decreases. Solar panels work by converting sunlight into electricity, and as the temperature rises, the efficiency of this conversion decreases.
- **Voltage Decrease :** The voltage of a solar panel decreases as its temperature increases. This is due to the fact that the semiconductor material in solar panels becomes less efficient at transporting charges as temperature increases.
- **Power Output Reduction :** Higher temperatures can lead to a decrease in the power output of solar panels. This is because the decrease in efficiency and voltage negatively impacts the overall power output.
- **Thermal Degradation :** High temperatures can cause thermal degradation of solar panel materials over time, reducing their lifespan and efficiency.
- **Operating Temperature Range :** Solar panels are designed to operate within a certain temperature range. If temperatures exceed this range, the performance of the panels can be further compromised.

Overall, while solar panels still generate electricity on hot days, their efficiency decreases as temperatures rise, impacting their overall performance and output.

I.7. Advantages and Disadvantages of PV Energy :

I.7.1. Advantages :

- **Renewable Energy** : Solar energy is an abundant and widely available renewable resource worldwide, making it a sustainable long-term energy source.
- **Low Greenhouse Gas Emissions** : Solar energy does not produce greenhouse gases during its use, helping to reduce carbon emissions and mitigate climate change.
- **Decreasing Costs** : The costs of solar technologies have significantly decreased over the years, making solar energy increasingly competitive compared to conventional energy sources.

- **Energy Independence** : Photovoltaic systems allow users to produce their own electricity, reducing their dependence on energy suppliers and market price fluctuations.
- **Low Maintenance** : Solar installations require minimal maintenance once installed, reducing long-term maintenance costs.

I.7.2. Disadvantages:

- **Sunlight Variability** : Solar energy depends on the availability of sunlight, making photovoltaic electricity production variable and intermittent, often requiring energy storage or integration with other energy sources.
- **High Initial Costs** : Although the costs of solar technologies have decreased, initial investments in solar installations can still be relatively high.
- **Environmental Impact**: While solar energy is generally considered clean, the manufacturing and disposal of solar panels can have an environmental impact.
- **Space Requirement** : Solar installations often require large land or roof areas to accommodate solar panels, which can pose challenges in densely populated urban areas or areas with limited space.
- **Dependency on Weather Conditions** : Solar system performance can be affected by weather conditions such as clouds, rain, or snow, which can reduce the efficiency of solar electricity production at certain times.

I.8. Conclusion :

In conclusion, this chapter covered the fundamentals of solar radiation and photovoltaic energy conversion. It explained how solar cells harness the photovoltaic effect to generate electricity from sunlight. The modeling and characteristics of photovoltaic generators were discussed, including factors influencing their efficiency like temperature and load resistance. Different types of photovoltaic cells based on silicon crystal structure were presented. The chapter also touched upon the components of photovoltaic modules and highlighted the key advantages and disadvantages of solar photovoltaic technology.

Chapter II

DC-DC Converter

II.1. Introduction :

DC-DC converters are essential electronic circuits that play a critical role in modern power management systems. Their primary function is to convert the voltage of a direct current (DC) source from one level to another, ensuring stable and efficient power delivery to various electronic devices and systems. In applications where input voltage levels can fluctuate due to factors such as battery discharging over time or changes in load conditions, DC-DC converters maintain a constant output voltage, providing reliable power to the system's components. One significant advantage of DC-DC converters is their superior power conversion efficiency. By using switching techniques, they can minimize power losses associated with resistive elements, such as transformers or linear regulators, which typically generate heat and waste energy. This results in better overall efficiency and prolonged battery life in portable devices. Moreover, DC-DC converters offer the flexibility to step up or down voltage levels, allowing for efficient power distribution management in electronic systems. They can also provide galvanic isolation, separating the input and output grounds to reduce the risk of ground loops and safeguard sensitive components from voltage spikes and noise.

II.2. DC-DC Converters :

The DC-DC converters are static converters powered by a DC voltage source, producing an adjustable DC voltage across a load.

The DC-DC converters can be built based on thyristors for high powers (several 100 MW with a chopping frequency of a few kHz).

Alternatively, they can be constructed using transistors for lower powers (several hundred kilowatts, up to 100 kW), with a high chopping frequency of up to 100 kHz.

The following figure illustrates the symbol of a DC-DC converter.

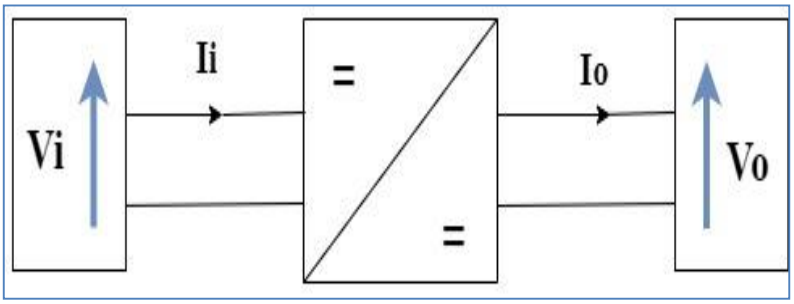

Figure (II.1): DC-DC Converters

II.3. Applications of DC-DC Converter :

For several years, switch-mode power converters have been used extensively in modern electronics technology across multiple sectors, including industrial, commercial, utility, and consumer markets. For low-power DC-DC conversion-based applications, most modern power conversion is accomplished using three major types of power converters – buck, boost, and buck-boost. However, specialized applications use advanced combinations or enhanced variations of the conventional types. There are several DC-DC converter types in the literature, but there is no one solution that caters to all the applications. Conversion techniques, in general, have found a wide array of applications in industry, research and development, and daily life[4].

DC-DC converters form a key aspect of study in the field of power electronics and energy drives as they are widely incorporated in several industrial applications. Some of the applications are illustrated in Figure (II.2). High voltage gain converters are employed in multiple sophisticated applications, including radar systems, DC distribution systems, data centers, and harnessing renewable energy[5].

This is especially crucial in the case of renewable energy applications as high voltage gain DC-DC converters facilitate boosting of the voltage that makes it suitable for integration with the distribution system. DC distribution in general offers a multitude of advantages including a reduced number of conversion units, price, and enhanced power quality, making it a preferred choice for a good range of applications.

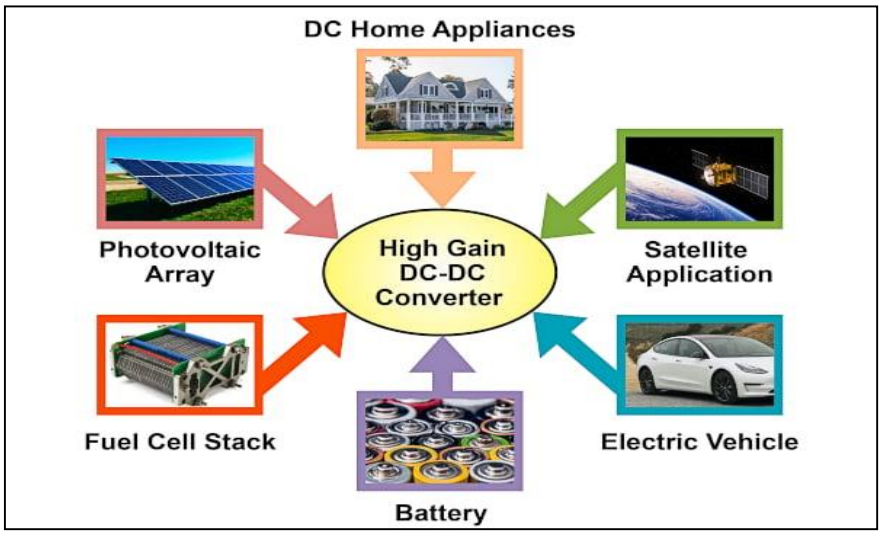

Figure (II.2): Applications of DC/DC Converters.

Here are some of DC-DC converter applications :

- **Renewable energy applications :** The DC-DC converter types employed for renewable energy applications need to draw continuous and smooth input current so ripple reduction can be achieved. It should also be able to integrate with different types of power sources. Non-isolated interleaved high voltage gain types are typically employed for interfacing renewables and microgrids[6]**.**
- **Medical devices :** Isolated DC-DC converters are crucial in applications where safety is a critical aspect. This is essential for separating the output from dangerous voltages on the input side. However, non-isolated converter types can be employed for applications like the power supply of an x-ray system.
- **Vehicles :** In the case of vehicles, the main DC-DC converter changes power from the onboard high voltage battery into lower DC voltages used to power lights, wipers, and window controls [7]**.** This is true for both electric vehicles and hybrid electric vehicles. Isolation is crucial in cases where separation of control systems is essential from high voltage domains. Buck-boost converters are utilized for step-up or step-down, and charge-pump converters are used for voltage inversion.
- **Smart lighting :** Several lighting applications require LED backlight driver solutions that possess high efficiency, direct current control, voltage protection, PWM-based control, and simple design. The DC-DC converter types that serve as effective drivers include linear regulators, charge pumps, and other conventional switching converters.

II.4. Types of DC-DC converters :

There are three types of DC-DC converters, namely: Buck, Boost, and Buck-Boost.

II.4.1. Buck Converter :

Buck Converter is a type of DC-DC converter that is designed to perform step-down conversion of the applied dc input signal. In the case of buck converters, the fixed dc input signal is changed into another dc signal at the output which is of lower value. This means it is designed to produce a dc signal as its output that possesses a lower magnitude than the applied input. It is sometimes called Step-down DC to DC Converter or Step-down Chopper or Buck Regulator.

Operating Principle of Buck Converter

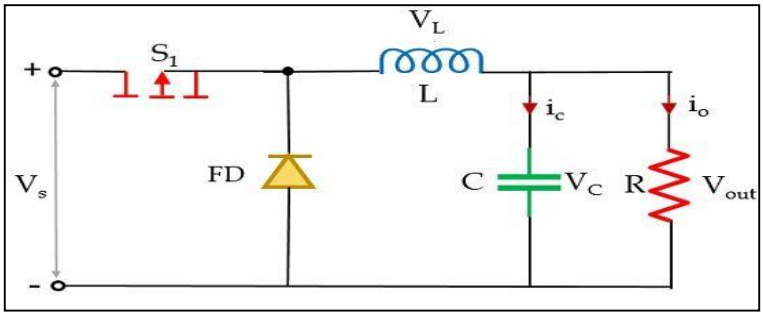

Figure (II.3): The Circuit Representation of Buck Converter

In the above figure, it is clearly shown that along with the power electronics solid-state device which acts as a switch for the circuit, there is another switch in the circuit which is a freewheeling diode. The combination of these two switches forms a connection with a low-pass LC filter in order to reduce current or voltage ripples. This helps in generating regulated dc output. A pure resistor is connected across this whole arrangement that acts as a load of the circuit.

The whole operation of the circuit takes place in two modes. The first mode is the one when the power MOSFET i.e., switch S_1 is closed.

In this mode of operation, switch S_1 is in closed condition thus allows the flow of current to take place through it.

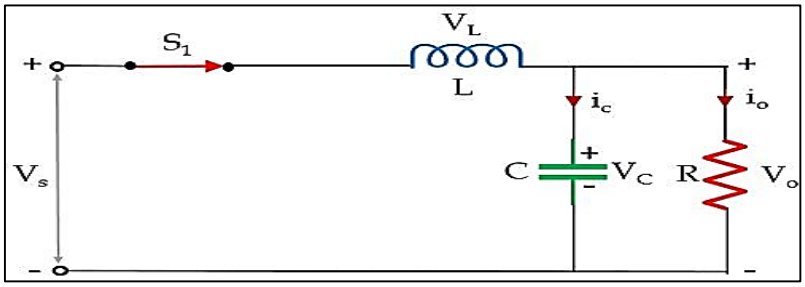

Figure (II.4): Buck Converter When S_1 is Closed

Initially when a fixed dc voltage is applied across the input terminal of the circuit then in the closed condition of switch S_1 current flows in the circuit in the manner shown above. Due to this flowing current, the inductor in the path stores energy in the form of a magnetic field. Also, there is a capacitor in the circuit and current flows through it also, therefore, it will store the charge and the voltage across it will appear across the load.

However, due to Lenz's law, the energy stored within the inductor will oppose the cause which has produced it and so an induced current will get generated and the polarity across the inductor will get reversed.

Here the total time period is a combination of T_{on} and T_{off} time.

$$\boldsymbol{T = T_{on} + T_{off}} \quad (\mathbf{II.1})$$

The duty cycle is written as:

$$\boldsymbol{D = \frac{T_{on}}{T}} \quad (\mathbf{II.2})$$

On applying KVL, in the above-given circuit

$$\boldsymbol{V_s = V_L + V_{out}} \quad (\mathbf{II.3})$$

$$\boldsymbol{V_L = V_s - V_{out}} \quad (\mathbf{II.4})$$

Also,

$$\boldsymbol{V_L = L\frac{di_L}{dt} = V_s - V_{out}} \quad (\mathbf{II.5})$$

$$\boldsymbol{\frac{di_L}{dt} = \frac{V_s - V_{out}}{L}} \quad (\mathbf{II.6})$$

When S1 is in closed condition then T_{on} = DT thus Δt = DT. Therefore, we can write

$$\boldsymbol{\frac{\Delta i_L}{\Delta t} = \frac{V_s - V_{out}}{L}} \quad (\mathbf{II.7})$$

$$\boldsymbol{\frac{\Delta i_L}{DT} = \frac{V_s - V_{out}}{L}} \quad (\mathbf{II.8})$$

Hence,

$$\boldsymbol{\Delta i_t = \left(\frac{V_s - V_{out}}{L}\right) DT} \quad (\mathbf{II.9})$$

The above equation represents the change in current through the circuit when switch S1 is closed.

Now, the second mode of operation takes place when switch S_2 is closed and S_1 gets open. However, you must be thinking about how automatically, the switch S_2 will be closed. So, as we have discussed that the inductor in the circuit will store the energy so, once S_1 will get open the inductor in the circuit will start acting as the source. In this mode, the inductor releases the energy which is stored in the previous mode of

operation. As we have discussed that the polarity of the inductor will get reversed therefore this causes the freewheeling diode to come in a forward-biased state which was earlier present in a reverse-biased state due to the applied dc input.

Due to this, the flow of current takes place in a way as shown below:

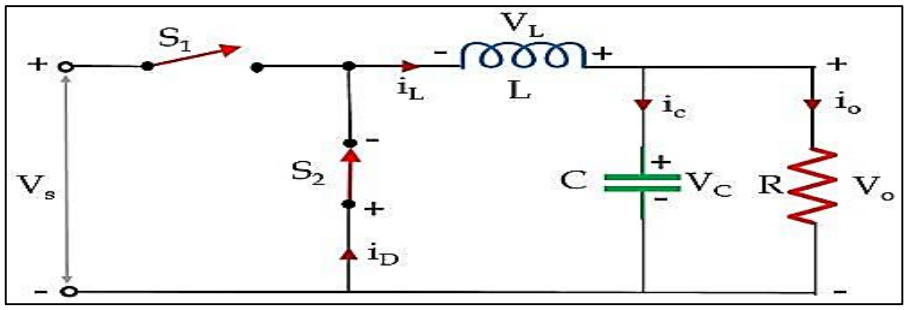

Figure (II.5): Buck Converter When S_2 is Closed

This flow of current will take place till the time the stored energy within the inductor gets completely collapsed. As once the inductor gets completely discharged, the diode comes in reverse biased condition leading to cause opening of switch S_2, and instantly switch S_1 will get closed and the cycle continues.

Now, let us apply KVL, in the above circuit

$$\mathbf{0} = \boldsymbol{V_L} + \boldsymbol{V_{out}} \quad \textbf{(II. 10)}$$

$$\boldsymbol{V_L} = \boldsymbol{L}\frac{\boldsymbol{di_L}}{\boldsymbol{dt}} = -\boldsymbol{V_{out}} \quad \textbf{(II. 11)}$$

Since, we know,

$$\mathbf{T} = \mathbf{T_{on}} + \mathbf{T_{off}} \quad \textbf{(II. 12)}$$

$$\mathbf{T} = \mathbf{DT} + \mathbf{T_{off}} \quad \textbf{(II. 13)}$$

$$\mathbf{T_{off}} = \mathbf{T} - \mathbf{DT} \quad \textbf{(II. 14)}$$

$$\mathbf{T_{off}} = (\mathbf{1} - \mathbf{D})\mathbf{T} \quad \textbf{(II. 15)}$$

$$\boldsymbol{V_L} = \boldsymbol{L}\frac{\boldsymbol{\Delta i_L}}{\boldsymbol{\Delta t}} = -\boldsymbol{V_{out}} \quad \textbf{(II. 16)}$$

$$\mathbf{T_{off}} = \mathbf{\Delta t} = (\mathbf{1} - \mathbf{D})\mathbf{T} \quad \textbf{(II. 17)}$$

$$\boldsymbol{L}\frac{\boldsymbol{\Delta i_L}}{(\boldsymbol{1} - \boldsymbol{D})\boldsymbol{T}} = -\boldsymbol{V_{out}} \quad \textbf{(II. 18)}$$

So,

$$\Delta i_L = -\frac{V_{out}}{L}(1-D)T \quad \text{(II. 19)}$$

This equation represents the rate of change in current through the inductor when the switch S1 is open.

As we know that the net change of current through the inductor in one complete cycle is zero. Thus,

$$\Delta i_{L_{(s1-closed)}} + \Delta i_{L(S1-\text{ open})} = 0 \quad \text{(II. 20)}$$

$$\frac{V_s - V_{out}}{L} DT + \left\{-\frac{V_{out}}{L}(1-D)T\right\} = 0 \quad \text{(II. 21)}$$

On simplifying,

$$\frac{V_s DT}{L} - \frac{V_{out}\, DT}{L} - \frac{V_{out}\, T}{L} + \frac{V_{out}\, DT}{L} = 0 \quad \text{(II. 22)}$$

$$\left(\frac{V_s DT}{L}\right) = \frac{V_{out}\, T}{L} \quad \text{(II. 23)}$$

$$V_{out} = DV_s \quad \text{(II. 24)}$$

The figure given below represents the waveform representation of Buck Converter:

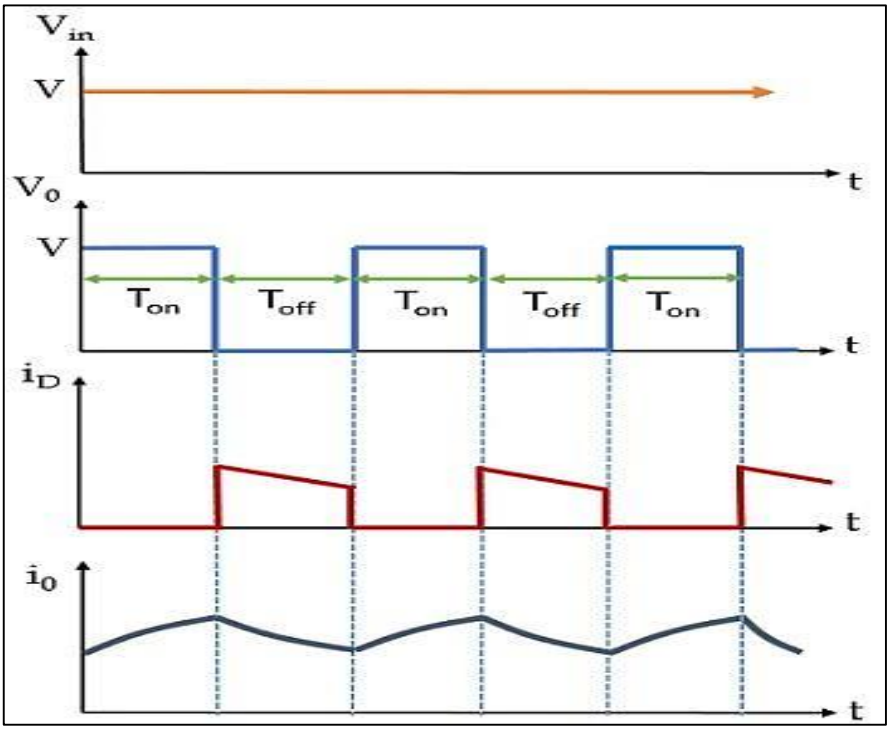

Figure (II.6): Waveform Representation

Hence, we can say, buck converters are used to provide a lower value of dc signal from a fixed dc input.

II.4.2. Boost Converter :

Boost Converters sometimes, also known as step-up DC-DC converters are the type of chopper circuits that provides such an output voltage that is more than the supplied input voltage. In the case of boost converters, the dc to dc conversion takes place in a way that the circuit provides a high magnitude of output voltage than the magnitude of the supply input. It is given the name 'boost' because the obtained output voltage is higher than the input voltage.

Operating Principle of Boost Converter

The figure given below is the circuit representation of the boost converter:

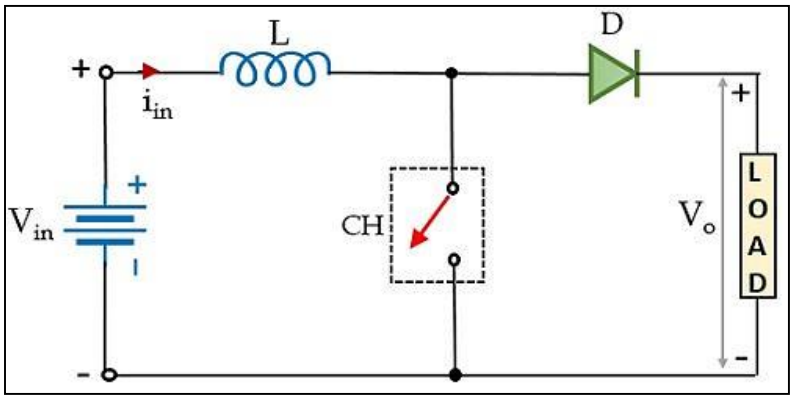

Figure (II.7): Elementary Circuit of Boost Converter

The circuit here is an elementary form of step-up DC-DC converter which necessarily requires a large inductor L in series connection with the voltage source. The whole circuit arrangement operates in a way that it helps in maintaining a regulated dc signal at the output.

Let us understand how the given circuit operates in order to provide an increased dc signal at the load.

Initially, when the chopper CH is in on state, then in the presence of supply dc input current begins to flow through the closed path of the circuit i.e., passing through the inductor as shown in the figure below.

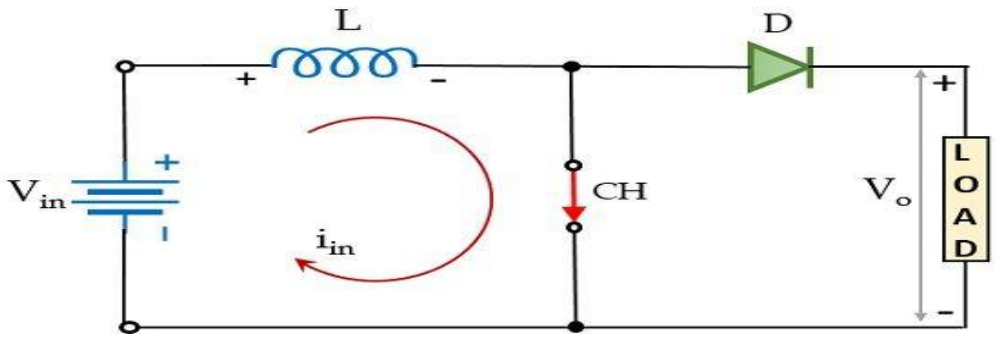

Figure (II.8): The Chopper CH is in on State

Here, the polarity of the inductor will be according to the direction of the flow of current. In this particular case, the diode in the configuration is in reverse biased condition and so current will not be allowed to flow through that particular part of the circuit during on state of the DC-DC converter. Resultantly, the voltage across DC-DC converter will appear across the load.

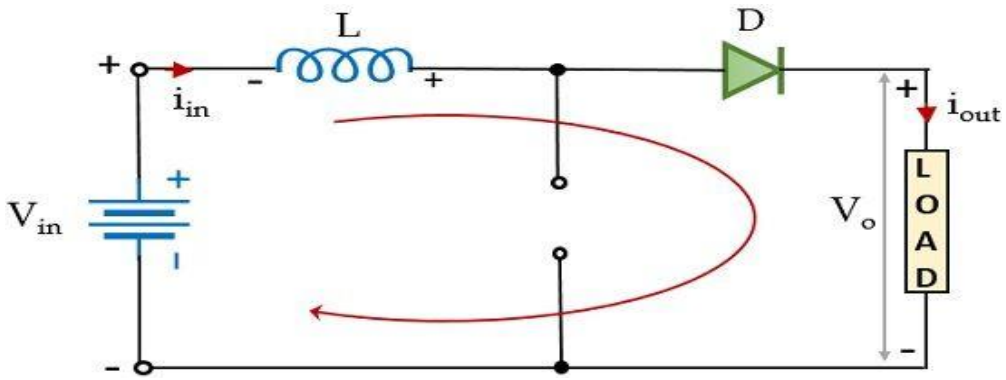

Figure (II.9): The Chopper CH is in Off State

Furthermore, at the instant when CH is in the off state, then the part of the circuit through which the current was flowing earlier will not be active in this case. However, as the inductor stores, the energy in the form of a magnetic field and so the current through it will not die out instantly.

Also, we know according to Lenz's law a reverse current will be induced that will oppose the cause which has produced it. And so, due to the induced current, the polarity of the inductor will get reversed. This reverse polarity of the inductor forward biases the diode present in the circuit. This provides the path for the current through the diode that flows through the load during the off state of the chopper i.e., T_{off}. However, we must note here that the current through the inductor is of decreasing nature and will die out after a point in time.

Thus, the total voltage across the load will be given as:

$$\boldsymbol{V_{out} = V_{in} + V_L} \qquad (\mathbf{II.25})$$

This means that the output voltage exceeds the applied input voltage. Thus, performs step-up conversion as the energy stored within the inductor during the T_{on} period is released during the T_{off} period.

During the T_{on} period, the voltage across the inductor will be given as:

$$\boldsymbol{V_L = L\frac{di}{dt}} \qquad (\mathbf{II.26})$$

Let us have a look at the waveform representation of the step-up chopper shown below:

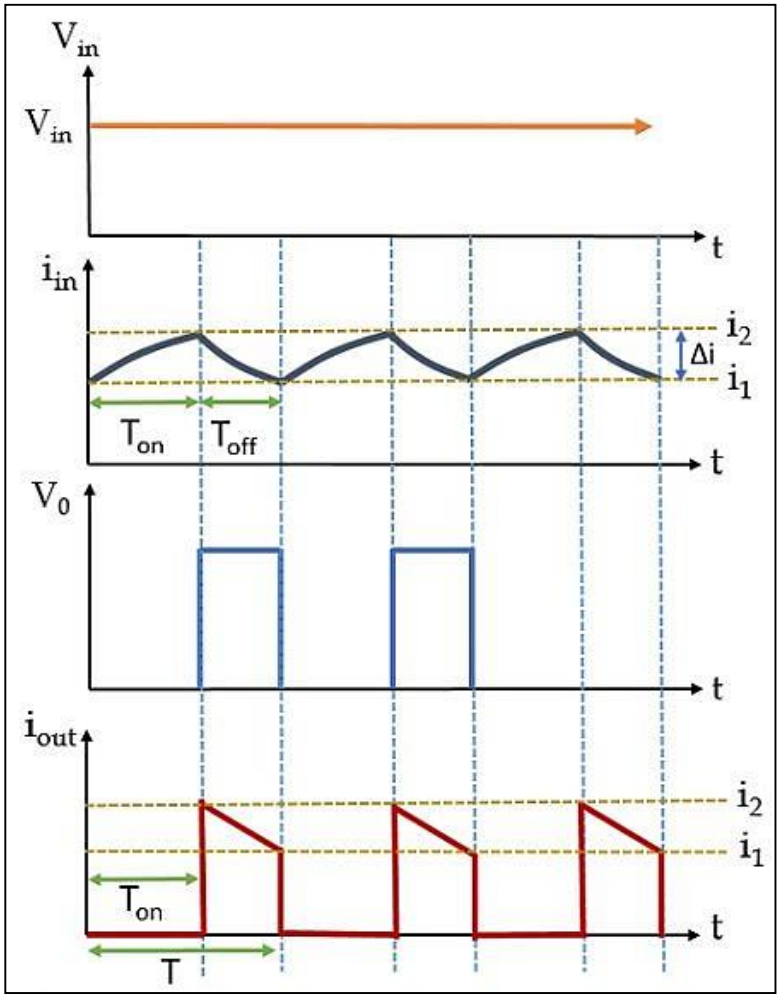

Figure (II.10): Waveform Representation

During the T_{on} period, the current through the inductor will change from i_1 to i_2 this is clearly shown above. While during the T_{off} period, the inductor current will change from i_2 to i_1. Now, talking about voltage, so during the turn-on period, the voltage across the inductor will be equal to the supply input voltage. But when CH gets off then on applying KVL in the figure shown above, we will get,

$$\boldsymbol{V_L - V_0 + V_{in} = 0} \quad \textbf{(II. 27)}$$

This means,

$$\boldsymbol{V_L = V_0 - V_{in}} \quad \textbf{(II. 28)}$$

Considering that output current is varying linearly, the energy input provided by the source to the inductor, when CH is on, is given as:

$\boldsymbol{W_{on}}$ = (**voltage across the inductor**)(**average current through the inductor**)$\boldsymbol{T_{on}}$

$$\boldsymbol{W_{on} = V_{in}\left(\frac{i_1 + i_2}{2}\right)T_{on}} \quad \textbf{(II. 29)}$$

Further, the energy that the inductor releases to the load when CH is off is given as:

$\boldsymbol{W_{off}}$ = (**voltage across the inductor**) **(average current through the inductor)** $\boldsymbol{T_{off}}$

$$\boldsymbol{W_{off} = V_{out} - V_{in}\left(\frac{i_1 + i_2}{2}\right)T_{off}} \quad \textbf{(II. 30)}$$

For a lossless system, comparing the two energies, we will have,

$$\boldsymbol{V_{in}\left(\frac{i_1 + i_2}{2}\right)T_{on} = V_{out} - V_{in}\left(\frac{i_1 + i_2}{2}\right)T_{off}} \quad \textbf{(II. 31)}$$

On simplifying,

$$\boldsymbol{V_{in}T_{on} = V_{out}T_{off} - V_{in}T_{off}} \quad \textbf{(II. 32)}$$

$$\boldsymbol{V_{out}T_{off} = V_{in}T_{on} + V_{in}T_{off}} \quad \textbf{(II. 33)}$$

$$\boldsymbol{V_{out}T_{off} = V_{in}(T_{on} + T_{off})} \quad \textbf{(II. 34)}$$

Since we know, $\mathbf{T = T_{on} + T_{off}}$, therefore,

$$\boldsymbol{V_{out}T_{off} = V_{in}T} \quad \textbf{(II. 35)}$$

$$\boldsymbol{V_{out} = V_{in}\frac{T}{T_{off}}} \quad \textbf{(II. 36)}$$

$$V_{out} = V_{in} \frac{T}{T - T_{on}} \quad (\text{II. 37})$$

$$V_{out} = V_{in} \frac{1}{\left(\frac{T}{T} - \frac{T_{on}}{T}\right)} \quad (\text{II. 38})$$

Since, we know, duty cycle i.e., $\alpha = T_{on}/ T$

$$V_{0ut} = V_{in} \frac{1}{(1 - \alpha)} \quad (\text{II. 39})$$

Thus, we can conclude here that the average load voltage can be stepped up with the change in the duty cycle.

II.4.3. Buck-Boost Converter :

The buck–boost converter is a type of DC-to-DC converter that has an output voltage magnitude that is either greater than or less than the input voltage magnitude. It is used to "step up" the DC voltage, similar to a transformer for AC circuits. It is equivalent to a fly-back converter using a single inductor instead of a transformer. Two different types are called buck–boost converter DC-DC converters, commonly referred to as choppers, include the versatile Buck-Boost converter. This converter can function as either a step-down or step-up converter, depending on its duty cycle, denoted as DA typical Buck-Boost converter circuit is shown below:

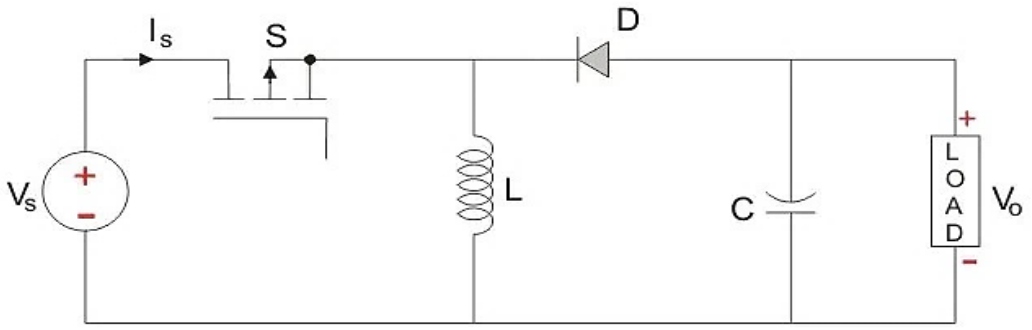

Figure (II.11): The Circuit Representation of Buck-Boost Converter

The input voltage source is connected to a solid-state device. The second switch used is a diode. The diode is connected, in reverse to the direction of power flow from source, to a capacitor and the load and the two are connected in parallel as shown in the figure above.

The controlled switch in the converter uses Pulse Width Modulation (PWM) to toggle on and off. PWM may operate based on time or frequency, with time-based being the more common approach.

Frequency-based modulation, though versatile, has the disadvantage of requiring a wide range of frequencies to precisely control the switch and thus achieve the desired output voltage.

Time based Modulation is mostly used for DC-DC converters. It is simple to construct and use.

The frequency remains constant in this type of PWM modulation. The Buck Boost converter has two modes of operation. The first mode is when the switch is on and conducting.

Mode I: Switch is ON, Diode is OFF

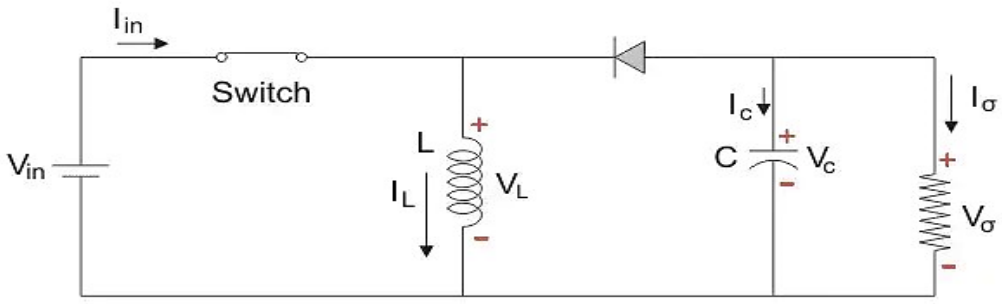

Figure (II.12): The Equivalent Circuit of Mode I

The Switch is ON and therefore represents a short circuit ideally offering zero resistance to the flow of current so when the switch is ON all the current will flow through the switch and the inductor and back to the DC input source.

The inductor stores charge during the time the switch is ON and when the solid state switch is OFF the polarity of the Inductor reverses so that current flows through the load and through the diode and back to the inductor. So, the direction of current through the inductor remains the same.

Let us say the switch is on for a time T_{ON} and is off for a time T_{OFF}.
We define the time period, T, as:

$$\boldsymbol{T = T_{ON} + T_{OFF}} \qquad (\mathbf{II.40})$$

and the switching frequency:

$$\boldsymbol{f_{\text{switching}} = \frac{1}{T}} \quad (\mathbf{II.41})$$

Let us now define another term, the duty cycle:

$$\boldsymbol{D = \frac{T_{ON}}{T}} \quad (\mathbf{II.42})$$

Let us analyse the Buck Boost converter in steady state operation for this mode using KVL.

$$\begin{gathered} \boldsymbol{V_{in} = V_L} \\ \boldsymbol{V_L = L\frac{di_L}{dt} = V_{in}} \\ \boldsymbol{\frac{di_L}{dt} = \frac{\Delta i_L}{\Delta t} = \frac{\Delta i_L}{DT} = \frac{V_{\text{in}}}{L}} \end{gathered} \quad (\mathbf{II.43})$$

Since the switch is closed for a time T_{ON} = DT we can say that Δt = DT.

$$\boldsymbol{(\Delta i_L)_{\text{closed}} = \left(\frac{V_{in}}{L}\right) DT} \quad (\mathbf{II.44})$$

While performing the analysis of the Buck-Boost converter we have to keep in mind that

- The inductor current is continuous and this is made possible by selecting an appropriate value of L.
- The inductor current in steady state rises from a value with a positive slope to a maximum value during the ON state and then drops back down to the initial value with a negative slope. Therefore, the net change of the inductor current over any one complete cycle is zero.

Mode II: Switch is OFF, Diode is ON

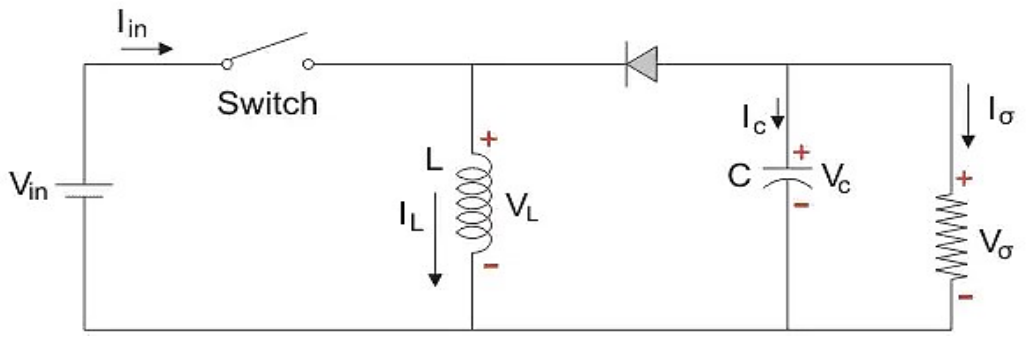

Figure (II.13): The Equivalent Circuit of Mode II

In this mode the polarity of the inductor is reversed and the energy stored in the inductor is released and is ultimately dissipated in the load resistance and this helps to maintain the flow of current in the same direction through the load and also step-up the output voltage as the inductor is now also acting as a source in conjunction with the input source. But for analysis we keep the original conventions to analyse the circuit using KVL.

Buck Boost Converter Formula

Let us now analyse the Buck Boost converter in steady state operation for Mode II using KVL.

$$\boldsymbol{V_L = V_o} \tag{II.45}$$

$$\boldsymbol{V_L = L\frac{di_L}{dt} = V_o} \tag{II.46}$$

$$\boldsymbol{\frac{di_L}{dt} = \frac{\Delta i_L}{\Delta t} = \frac{\Delta i_L}{(1-D)T} = \frac{V_o}{L}} \tag{II.47}$$

Since the switch is open for a time

$$\boldsymbol{T_{OFF} = T - T_{ON} = T - DT = (1-D)T} \tag{II.48}$$

we can say that

$$\boldsymbol{\Delta t = (1-D)T} \tag{II.49}$$

$$\boldsymbol{(\Delta i_L)_{\text{open}} = \left(\frac{V_o}{L}\right)(1-D)T} \tag{II.50}$$

It is already established that the net change of the inductor current over any one complete cycle is zero.

$$(\Delta i_L)_{\text{closed}} + (\Delta i_L)_{\text{open}} = 0 \qquad (\text{II. 51})$$

$$\left(\frac{V_o}{L}\right)(1-D)T + \left(\frac{V_{\text{in}}}{L}\right)DT = 0 \qquad (\text{II. 52})$$

$$\frac{V_o}{V_{\text{in}}} = \frac{-D}{1-D} \qquad (\text{II. 53})$$

We know that D varies between 0 and 1. If D > 0.5, the output voltage is larger than the input; and if D < 0.5, the output is smaller than the input. But if D = 0.5 the output voltage is equal to the input voltage[8].

II.5. Comparison of Converter Types :

Table (II.1) summarizes the voltage gains and switch stresses for the different converter types. For these converters, the evolution of the voltage gains as a function of the duty cycle is shown. While several types can be considered as boost converters, particularly if the duty cycle is greater than 0.5, only the boost type provides a boosting capability over the entire duty cycle range. For a duty cycle of 0.5 for example, the boost converter exhibits an output voltage twice the input voltage. Whereas for the other boost-derived type, the output voltage is equal to the input voltage for this duty cycle value. It is only when the duty cycle approaches 1 that the other boost-derived types tend to resemble the behavior of the conventional boost type.[9].

Converter /Parameters	Voltage Gain $\frac{Vout}{Vin}$	Voltage Controls $V_{k,max} = \lvert Vd,max \rvert$	Current Controls $i_{k,max} = V_{d,max} = i_{d,max}$
Boost	$\frac{1}{1-\alpha}$	$\frac{Vin}{1-\alpha} + \frac{\Delta Vout}{2}$	$\frac{Iout}{1-\alpha} + \frac{\Delta IL}{2}$
Buck	$\frac{\alpha}{1-\alpha}$	$\frac{Vin}{1-\alpha} + \frac{\Delta Vout}{2}$	$\frac{VC}{1-\alpha} + \frac{\Delta Vout}{2}$
Buck-Boost	α	Vin	$i_L + \frac{\Delta IL}{2}$

Table (II.1): Comparison of Converter Types.

II.6. Efficiency of Static Converters :

The table provides insight into the efficiency of some well-known converter types. [10]

Structure	Conversion Efficiency	Battery
Boost	92%	24V
Buck	93%	12V
Buck-Boost	92%	12-24V

Table (II.2): Efficiency of Static Converters.

II.7. Conclusion :

In conclusion, DC-DC converters play a crucial role in modern electronics, facilitating efficient power management by converting one voltage level to another. With various types such as buck, boost, buck-boost. They offer versatility in meeting the diverse voltage requirements of different electronic systems.

These converters find wide-ranging applications in industries such as automotive, renewable energy, telecommunications, and consumer electronics. From powering small electronic devices to managing energy flow in solar power systems, DC-DC converters are indispensable.

On a related note, Maximum Power Point Tracking (MPPT) is a vital technology, particularly in renewable energy systems such as solar power. It enables efficient extraction of maximum power from photovoltaic panels by adjusting the electrical operating point. In the following chapter we will delve into MPPT, its importance, and its various implementation methods.

Chapter III

Maximum Power Point Tracking

III.1. Introduction :

In order to overcome the performance issue of solar panels and achieve maximum efficiency, it is necessary to optimize the design of all parts of the PV system. Additionally, it is essential to optimize the DC/DC converters used as the PV generator input interface and the load in order to extract maximum power continuously and thus operate the PV system at its maximum power point (MPP) without loss in the transferred energy using a Maximum Power Point Tracking (MPPT) controller. Consequently, maximum power is obtained under varying load and atmospheric conditions (brightness and temperature).

A significant number of MPPT control techniques have been developed since the 1970s, starting with simple techniques such as MPPT controllers based on feedback of voltage and current states, to more efficient controllers using algorithms to calculate the PV system's MPP. Among the most commonly used techniques are the Incremental Conductance (INC) method, Perturb and Observe (P&O) method, and "hill climbing" method[11].

III.2. Maximum Power Point Tracking :

The enhancement of photovoltaic (PV) system efficiency necessitates the maximization of the PV generator power. This can be achieved by appropriately selecting the operating point, thereby adapting the load impedance to the voltage source. The DC-DC converter serves as an impedance adapter, thus ensuring operation at the optimal point, which enables the maximum power production of the PV generator[12].

Consequently, maximizing the power output of a photovoltaic source involves seeking this optimal operating point. This control is referred to as the maximum power point tracking (MPPT). These MPPT methods are based on iterative search algorithms to determine the operating point of the solar module so that the generated power is maximal without interrupting system operation. They are founded on the continual maximization of the power generated by the PV modules. The power extracted from the module is calculated based on the current and voltage measurements of the module and the multiplication of these two quantities. These measurements are utilized by various methods that pursue the real maximum power point (MPP). There are several types of MPPT controls, among which, we present the principles of a few MPPT

methods, such as the constant voltage method, the constant current method, the incremental conductance algorithm, and the perturbation and observation method. The latter method is employed in our work due to its ease of implementation.

III.3. Working principle of MPPT :

Specific control laws exist to bring devices to operate at maximum points of their characteristics without these points being known in advance, nor without knowing when they have been modified or what the reasons for this change are. For energy sources, this results in maximum power points. This type of control is often referred to in the literature as "Maximum Power Point Tracking" or "MPPT" in Anglo-Saxon (MPPT). The principle of these controls is to perform a search for the maximum power point (MPP) while ensuring a perfect adaptation between the generator and its load in order to transfer the maximum power[13].

To simplify the operating conditions of this control, a DC load is chosen. As we can see on this chain, the MPPT control is necessarily associated with a four-pole with degrees of freedom that allow adaptation between the PV generator and the load. In the case of solar conversion, the four-pole can be realized using a DC-DC converter so that the power supplied by the PV generator corresponds to the maximum power (P_{MAX}) that it generates and that it can then be transferred directly to the load.

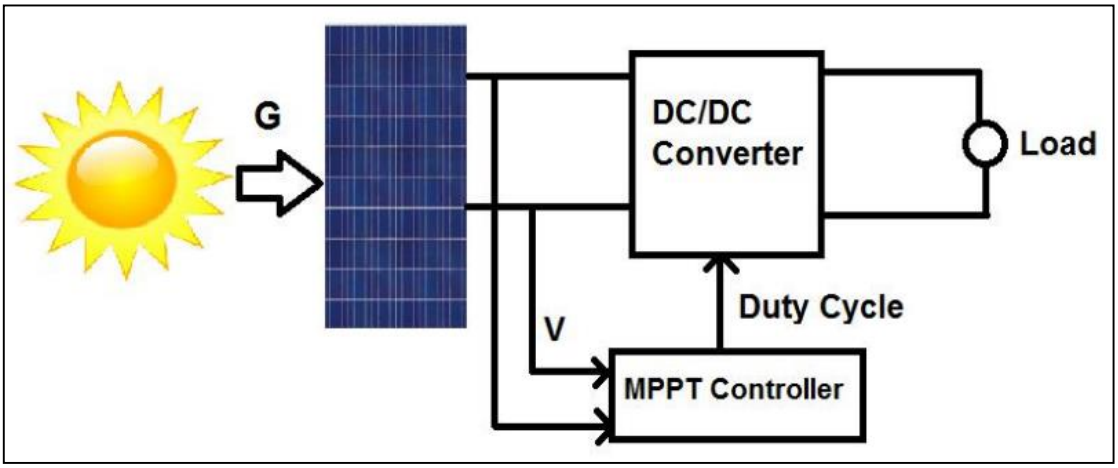

Figure (III.1): Block Diagram of The PV System

The commonly used control technique is to act on the duty cycle automatically to bring the generator to its optimum operating value because of sudden load variations that can occur at any time. Figure (III.2) illustrates three (03) sorts of disturbances. Depending on the type of disturbance, the operating point moves from the maximum

power point MPP1 to a new operating point P1 more or less far from the optimum. For a variation of sunshine (case a), one needs to adjust the duty cycle value to converge to the new MPP2. For a load variation (case b), we may note a change in the operating point which can find a new optimum position due to the action of a command. To a lesser extent, the last case of variation of the operating point may occur due to the variations in operating temperature of the photovoltaic module (case c). Although we have to act at the command level, the latter does not have the same time constraints as the previous two cases[14].

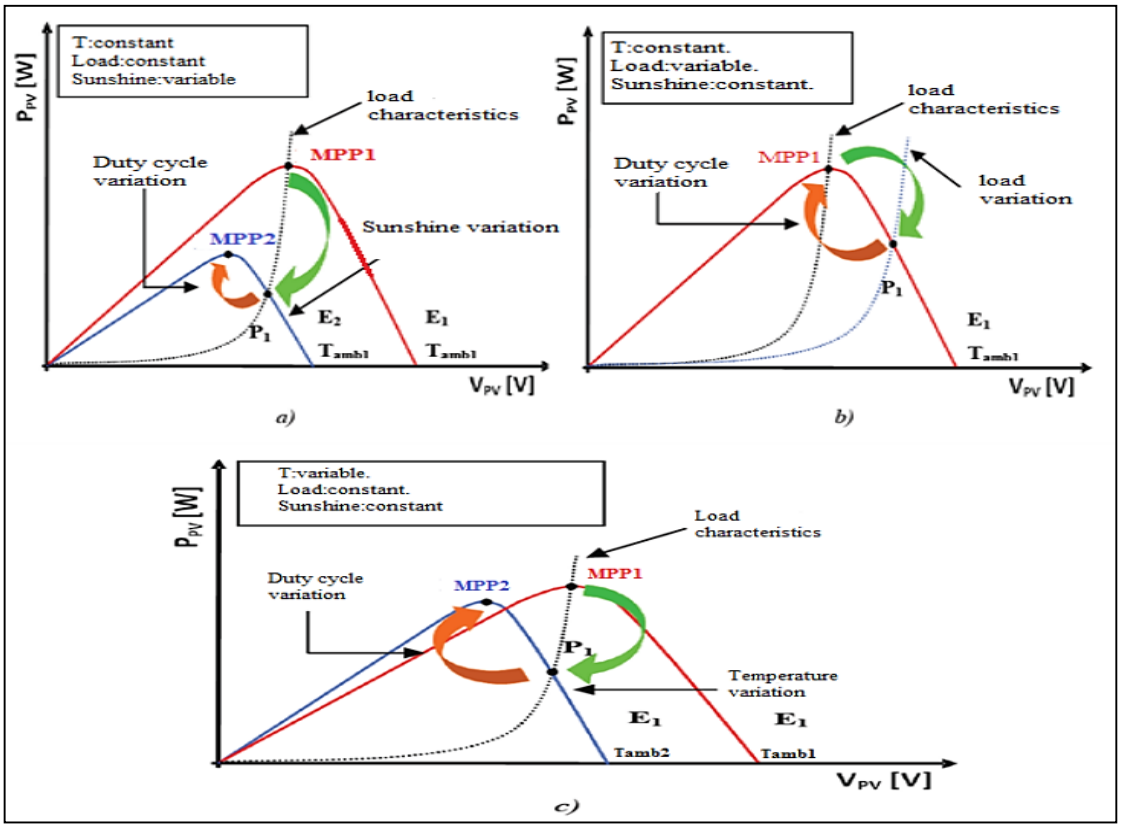

Figure (III.2): Search and Recovery Of MPP

III.4. Classification of MPPT Control :

We can generally classify MPPT controllers according to the type of electronic implementation: analogical, digital, or mixed. However, it is more interesting to classify them according to the type of search they perform and the input parameters of the MPPT controller.

III.4.1. Classification of MPPT Controllers Based on Input Parameters :

a) MPPT Controllers Operating from Input Parameters :

There are a number of MPPT controllers that perform a maximum power point search according to the evolution of the power supplied by the PV array. Examples include the Perturb and Observe method, incremental conductance algorithms that use the value of the power supplied by the PV array to apply an appropriate control action for MPP tracking, or controllers based on proportional relationships between the optimal parameters characterizing the maximum power point (V_{opt} and I_{opt}) and the characteristic parameters of the PV module (V_{oc} and I_{sc}).

Notably, MPPT controllers inspired by neural networks fall into this category. In these controllers, either large computer memory systems storing all possible cases are used, or the controllers are again approximate. All of these controllers have the advantages of precision and fast response time[15].

b) MPPT Controllers Operating from Output Parameters of the Converter :

In the literature, there are also algorithms based on the output parameters of the DC-DC converters. For example, MPPT controllers based on maximizing the output current, which are primarily used when the load is a battery. In all systems using the output parameters, an approximation of P_{max} is made through the efficiency of the converter. In summary, the better the conversion stage, the more valid this approximation is. However, in general, all single-sensor systems are inherently imprecise. Most of these systems were originally designed for space applications[15].

III.4.2. Classification of MPPT Controllers According to the Type of Search :

a) Indirect MPPT :

This type of MPPT control utilizes the existing link between the measured variables (or $\boldsymbol{V_{oc}}$), which can be easily determined, and the approximate position of the MPP. It also includes controls based on an estimation of the operating point of the PV system made from a predefined parametric model. There are also controls that establish optimal voltage tracking by only considering variations in cell temperature provided by a sensor. These controls have the advantage of being

simple to implement. They are mainly intended for inexpensive and imprecise systems operating in geographical areas with little climate change[16].

b) Direct MPPT :

This type of MPPT control determines the optimal operating point (MPP) based on the currents, voltages, or powers measured in the system. It can therefore react to unpredictable changes in the operation of the PV system. Generally, these procedures are based on a search algorithm, with which the maximum power point of the curve is determined without interrupting operation. To do this, the operating point voltage is incremented at regular intervals. If the output power is greater, then the search direction is maintained for the next step; otherwise, it is reversed. The actual operating point then oscillates around the MPP. This basic principle can be preserved by other algorithms against interpretation errors. These errors may occur, for example, due to a wrong search direction resulting from an increase in power due to a rapid increase in radiation levels. Determining the value of the PV generator power, essential for finding the MPP, requires measuring the generator's voltage and current, and multiplying these two variables. Other algorithms are based on introducing small-signal sinusoidal variations in the converter switching frequency to compare the alternating and direct components of the PV system voltage and thus place the PV system operating point as close as possible to the MPP. The advantage of this type of control is its precision and rapid reaction[16].

III.5. Different MPPT Commands Synthesis :

Various works on MPPT commands appear regularly in the literature since 1968, the date of publication of the first command law adapted to renewable energy (photovoltaic). Given the large number of publications in this field, we have a classification of different MPPT according to their basic principles.

III.5.1. First MPPT Commands Types :

The algorithm implemented in the first MPPT command was relatively simple. Indeed, the capacity of microcontrollers available at that time was low and applications, especially, for space had fewer constraints regarding temperature and solar irradiation. The first command to be applied to a photovoltaic system was described by A.F. Boehringer. The command was based on an algorithm of adaptive control, to maintain the system at its maximum power point PPM. This is described in Figure 3 and can be

easily implemented on a computer. The system calculates the power at time t_i from the measurements of I_{PV} and V_{PV}, and compares it to the one stored in memory (time t_i-1). From there, a new duty cycle D is calculated and applied to the static converter.

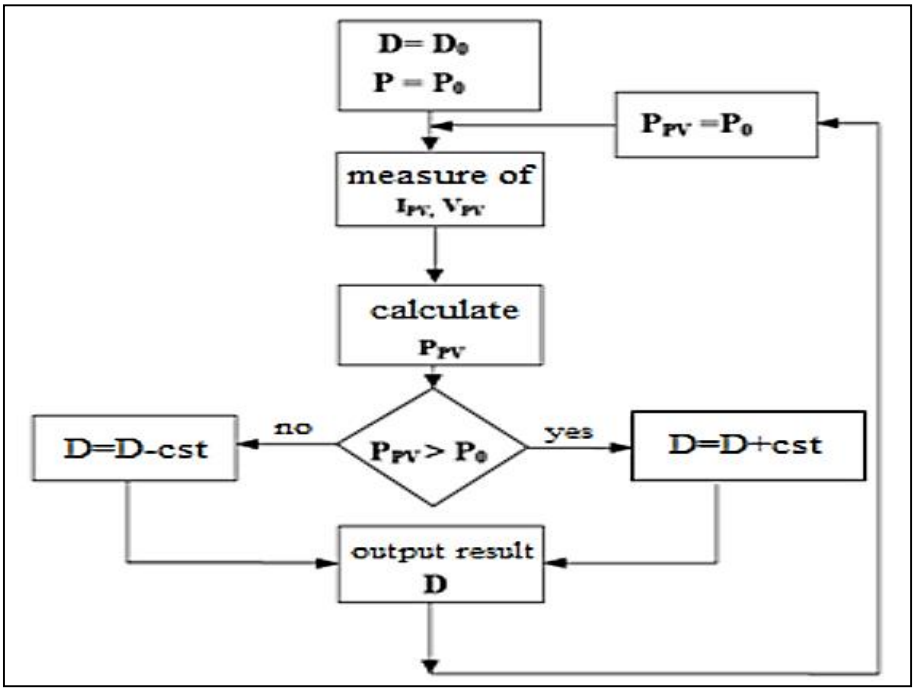

Figure (III.3): Bloc Diagram of a Digital MPPT Command

This principle is always valid from a theoretical point of view and applied nowadays to more efficient numerical algorithms. However, the response time has been improved as well as the PPM search accuracy[14].

III.5.2. Efficient MPPT Commands Algorithms :

The three (04) methods most commonly encountered are commonly referred to respectively as Hill Climbing, Perturb & Observe and Incremental Conductance and Artificial Neural Networks.

III.5.2.1. Algorithm Perturb and Observe (P&O) :

The principle of MPPT commands of P & O types is to disrupt the voltage V_{PV} with a low amplitude around its initial value and analyse the behaviour of the resulting power variation P_{PV}. Thus, as shown in Figure (III.4), we can deduce that if a positive increment of voltage V_{PV} generates an increase of power P_{PV}, this means that the operating point is to the left of the MPP. If, however, the power decreases, this implies that the system has exceeded the MPP.

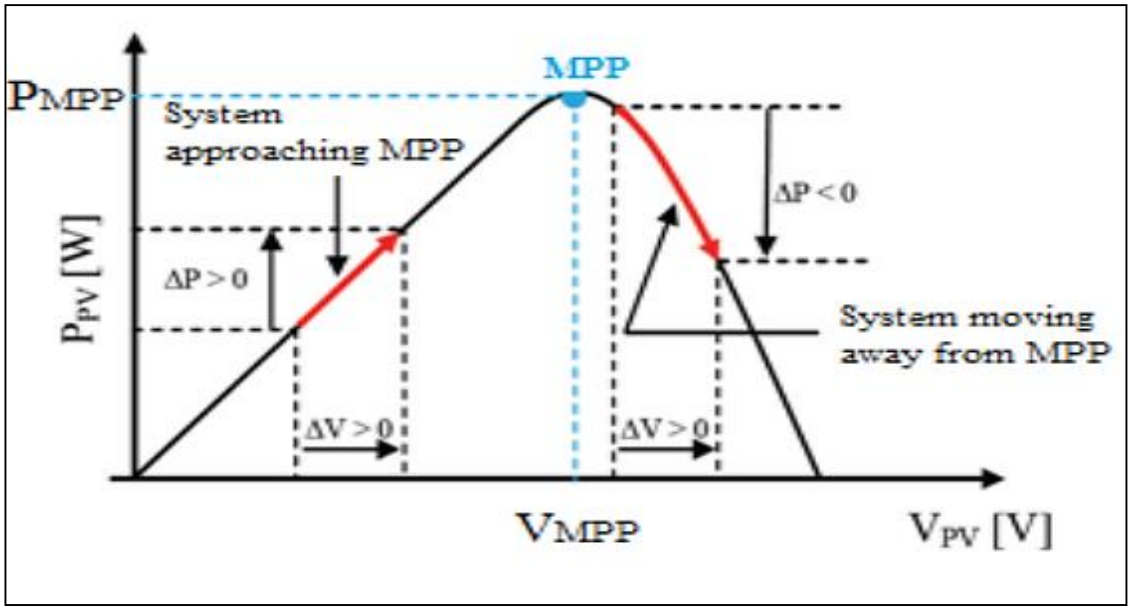

Figure (III.4): Ppv VS Vpv Characteristic of a Solar Panel

Figure (III.5) shows the algorithm associated with a conventional MPPT command of the P & O type, where the evolution of the power is analyzed after each voltage disturbance. For this type of command, two sensors (current and voltage) are needed to determine the power of the solar generator at every instant of time. The Perturb & Observe method is nowadays widely used because of its ease of implementation. However, it has some problems associated with oscillations around the MPP it generates in steady state because the search of the MPP should be repeated periodically, causing the system to oscillate continuously around the MPP.

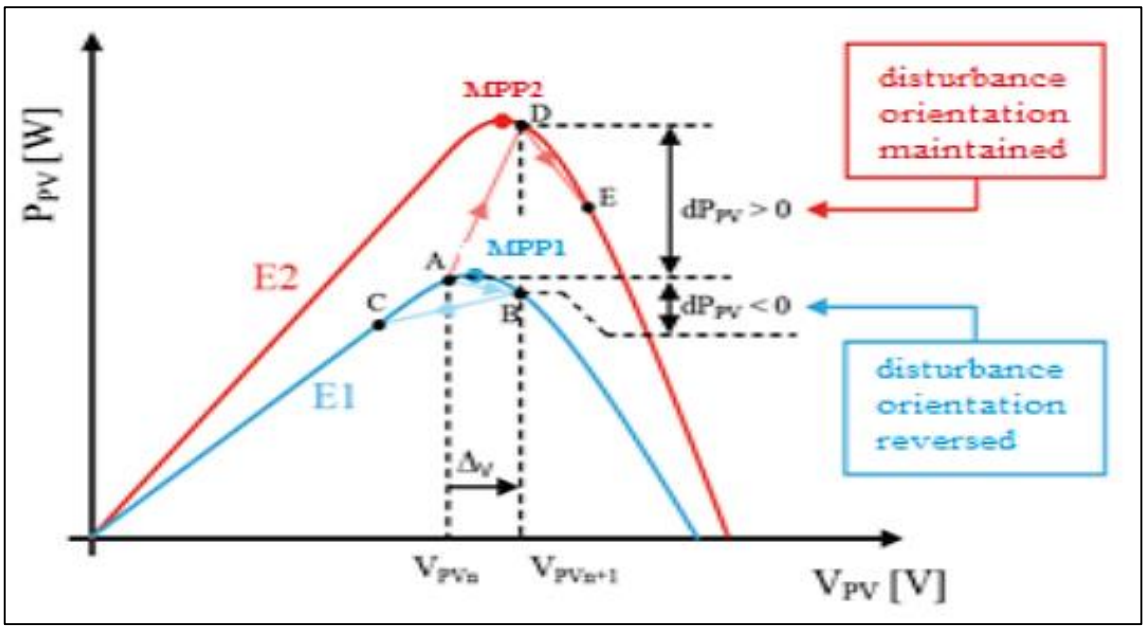

Figure (III.5): Divergence of The P & O Command Due to Radiation Variations

Figure (III.6) shows a detailed algorithm of the P & O command.

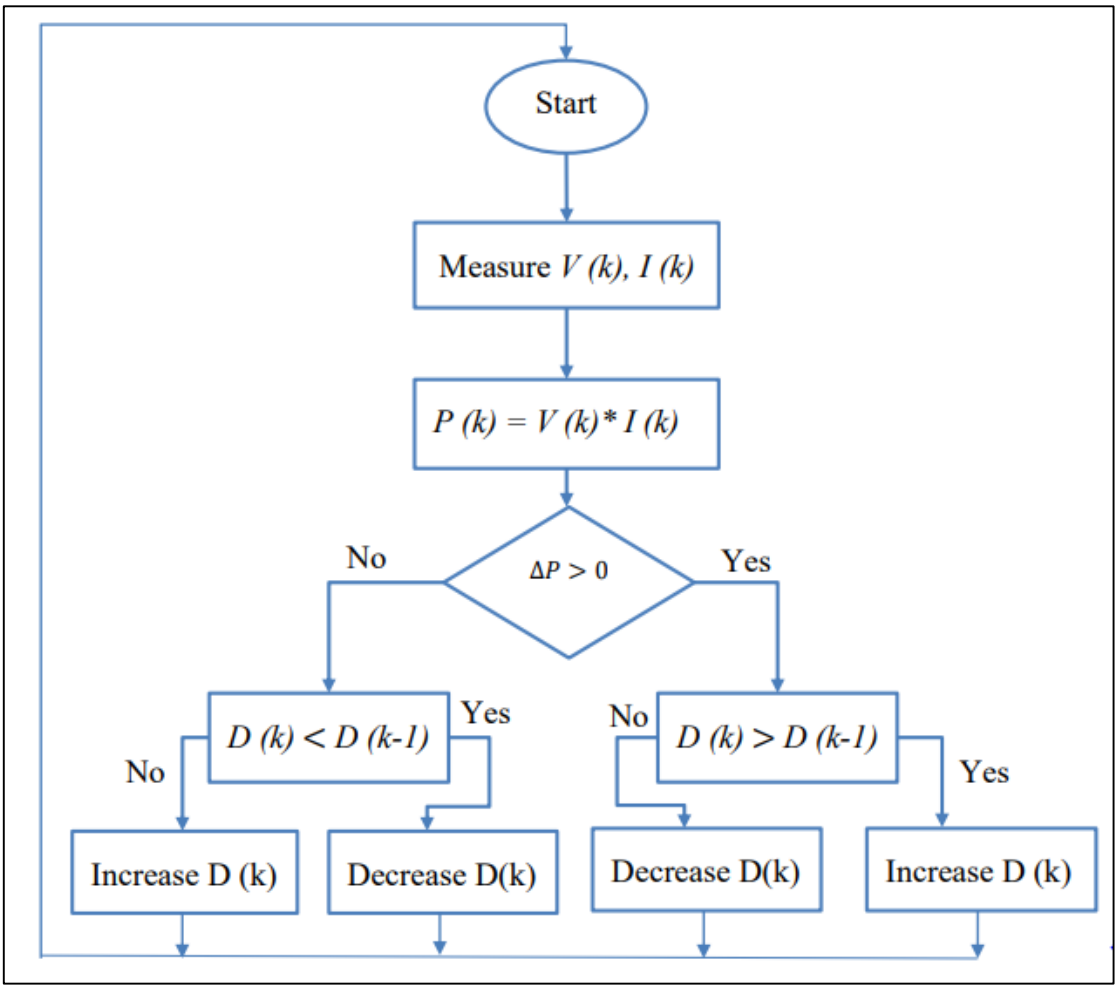

Figure (III.6): Algorithm of The P & O Type of Command

To understand this, consider the example of a given solar irradiation, E1, with an operating point lying in A. following a voltage disturbance of value ΔV, it switches to B, implying a variation of operating without illumination, a reversal of the sign of the disturbance due to the detection of a negative sign for the derivative of the power resulting, in equilibrium, in oscillations around the MPP due to the path of the operating point between points B and C. it can be noted that losses of power transfer will be more or less important depending on the respective positions of points B and C with respect to A. When changing the irradiation of the module from E1 to E2, the operating point then moves from A to D, which is interpreted in this case as a positive power variation[14].

III.5.2.2. Algorithm Hill Climbing :

The best thing about the hill climbing MPPT method is its simplicity. It uses the duty cycle of the boost converter as feedback parameter when the task of the MPPT is carried out[17],[18]. The main disadvantage of this technique is due to the trade-off between the stability of the system in a period of constant irradiation. Another disadvantage is the absence of a rapid response in case of a rapid change in radiation[17],[18]. The period of steady radiation requires a very small value of variation in the duty cycle, ΔD to avoid a strong oscillation of the power about the peak power point, reducing the energy captured by the PV. On the other hand, rapidly changing irradiation requires a higher duty cycle value to accelerate the pursuit of peak power.

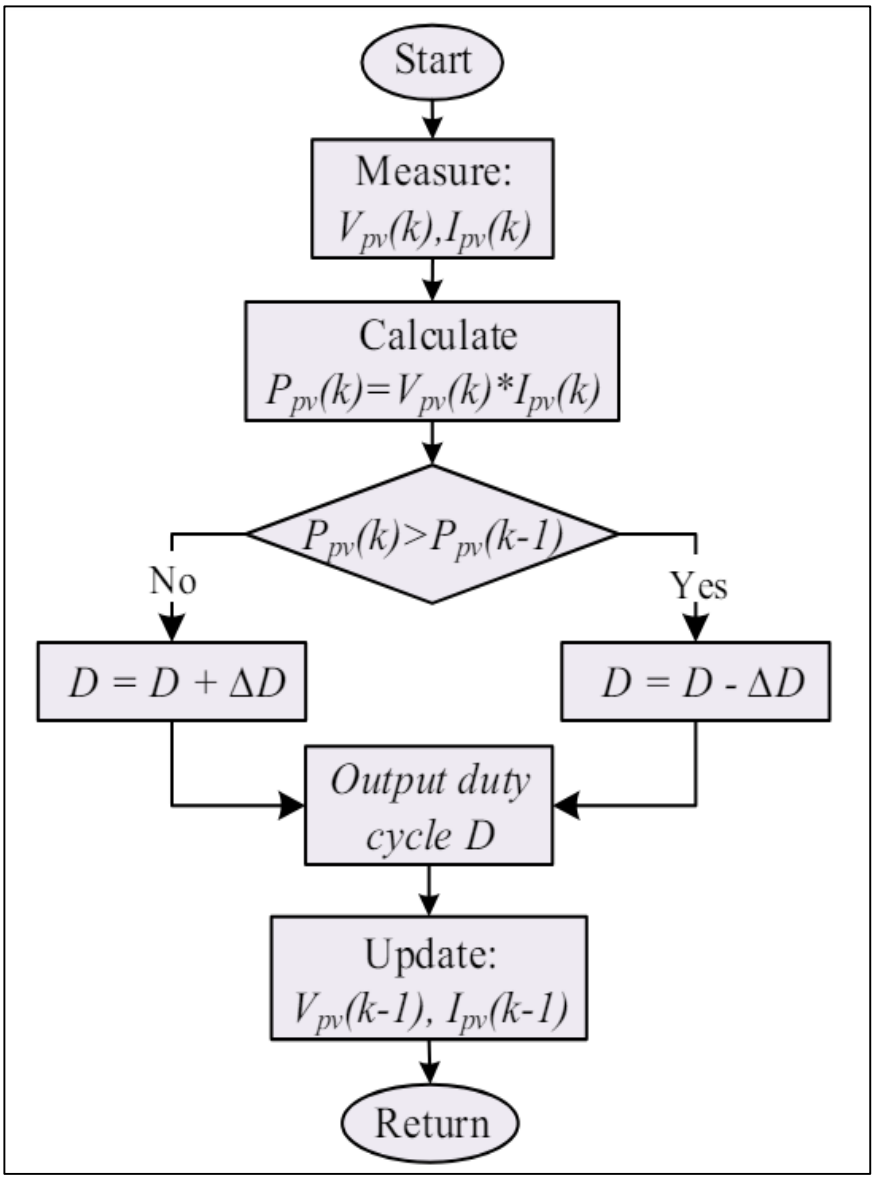

Figure (III.7): State Flowchart of Hill Climbing MPPT Technique.

III.5.2.3. Algorithm Incremental conductance (INC) :

The principle of this algorithm is based on knowledge of the conductance value G=I/V and the conductance increment (dG) in order to deduce the position of the operating point relative to the maximum power point. If the conductance increment (dG) is greater than the negative of the conductance (-G), the duty cycle is decreased. On the other hand, if the conductance increment is less than the negative of the conductance, the duty cycle is increased. This process is repeated until the maximum power point is reached[19].

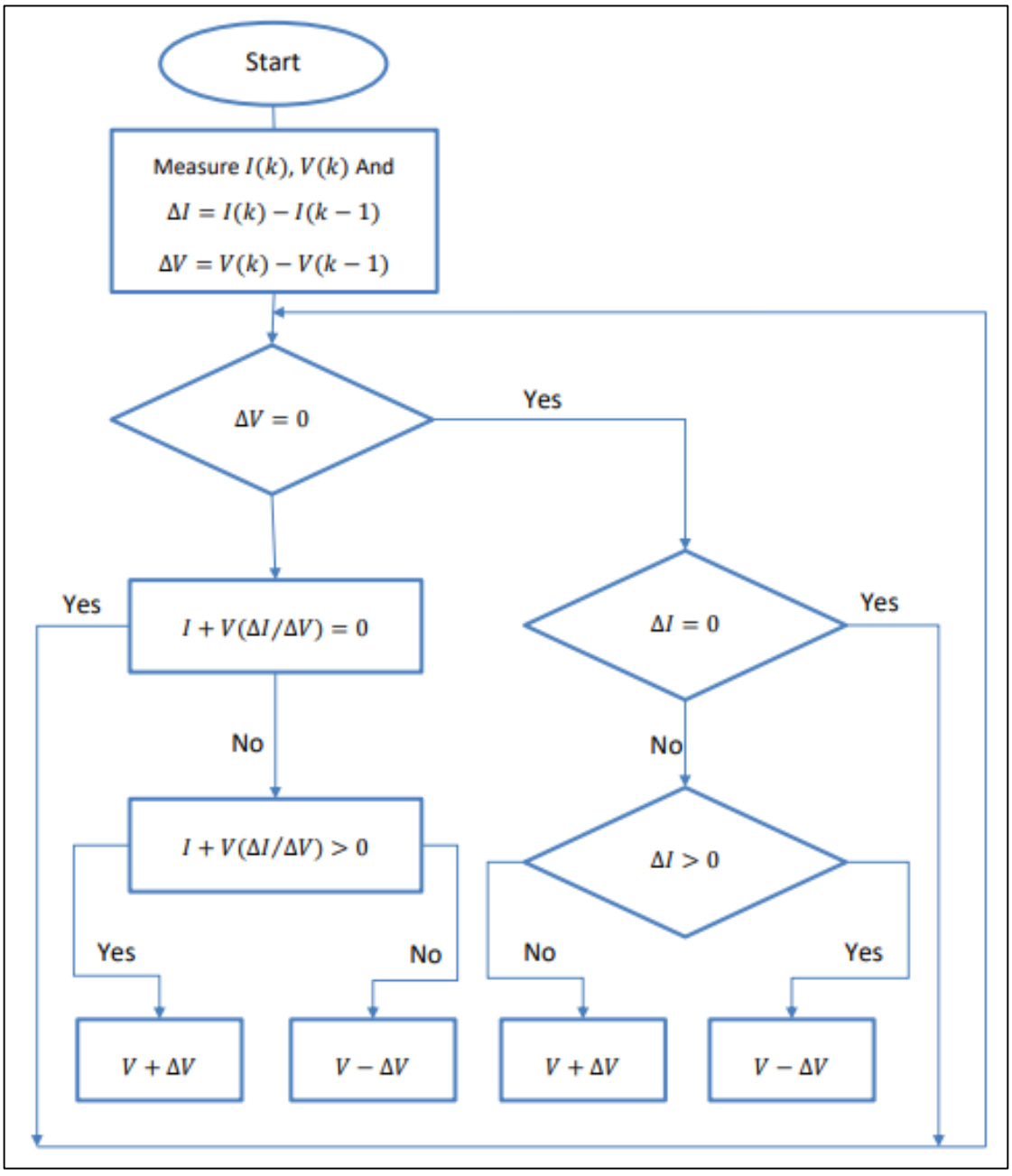

Figure (III.8): Flowchart for The Incremental Conductance Algorithm.

III.5.2.4. Artificial Neural Networks (ANN) :

Generally, an artificial neural network utilizes numerous processors working simultaneously and arranged in different layers. The initial layer takes in raw data inputs, similar to how the optic nerves receive visual information in humans.

Afterward, each subsequent layer receives the processed outputs from the previous layer. This process resembles the human experience, where neurons receive signals from neurons closer to the optic nerve. The final layer, however, generates the system's ultimate results or outputs.

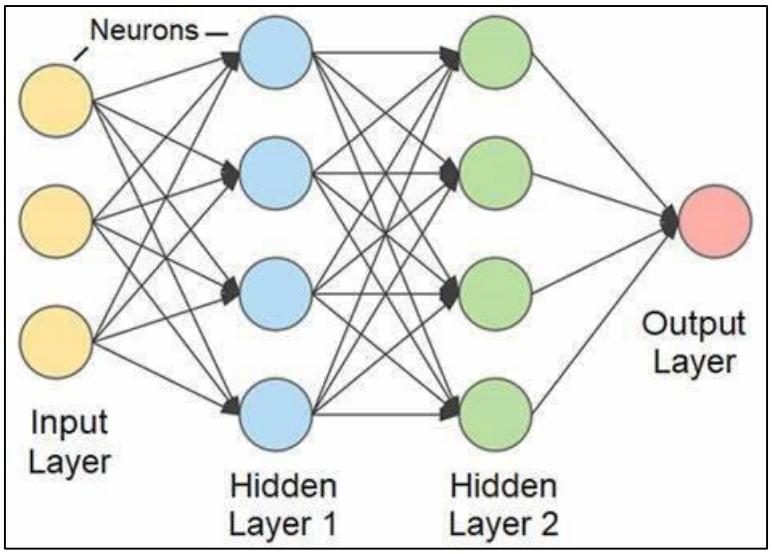

Figure (III.9): Functioning of Artificial Neural Networks

Neural networks enable computers to learn from new data through algorithms. Computers with neural networks are trained on labeled example data to learn tasks like object recognition by analyzing patterns in the examples. Unlike traditional algorithms, neural networks cannot be directly programmed - they learn in a similar way to a child's developing brain. There are three main learning methods:

1. **Supervised Learning :** The algorithm trains on labeled data and adjusts until it can achieve the desired output.
2. **Unsupervised Learning :** The network analyzes unlabeled data, with a cost function guiding it towards the desired result by indicating deviations.
3. **Reinforcement Learning :** The network is rewarded for positive results and penalized for negative ones, enabling it to learn and improve over time like humans learn from mistakes.

III.5.2.4.1. Application of Artificial Neural Networks in MPPT :

Artificial neural networks are employed to optimize maximum power point tracking (MPPT), a crucial element in photovoltaic (PV) systems. They improve the efficiency of capturing solar energy by continuously adjusting the operating point of the PV panels to maximize their power output. This adjustment accounts for changing environmental factors like solar radiation levels, temperature, and shading conditions. By doing so, neural network-based MPPT enables PV systems to more effectively harness solar energy and increase their overall energy production.

This example shows the use and practical application of artificial neural networks and their valuable role in improving the performance of PV systems through MPPT algorithms[20].

III.5.2.4.2. Implementation of ANN in MATLAB/SIMULINK :

The Neural Network Fitting app in MATLAB provides a user-friendly interface for designing, training, and evaluating artificial neural networks. The process involves selecting the data, configuring the network architecture, training the network, and assessing its performance through various plots and metrics. This tool is particularly useful for tasks like MPPT, where accurate modeling of complex relationships between inputs and outputs is crucial.

1. Data Collection :

The initial phase of the proposed method involves collecting data from MPPT method simulations performed under a variety of scenarios. Data collection is the cornerstone for training and evaluating the ANN-based MPPT model[20].

2. Setting Up the Neural Network Fitting Tool :

To begin the implementation process, we will open the Neural Network Fitting Tool in MATLAB. This tool provides a user-friendly interface for training and evaluating neural networks. We will import our defined variables and configure the tool for our specific application[21].

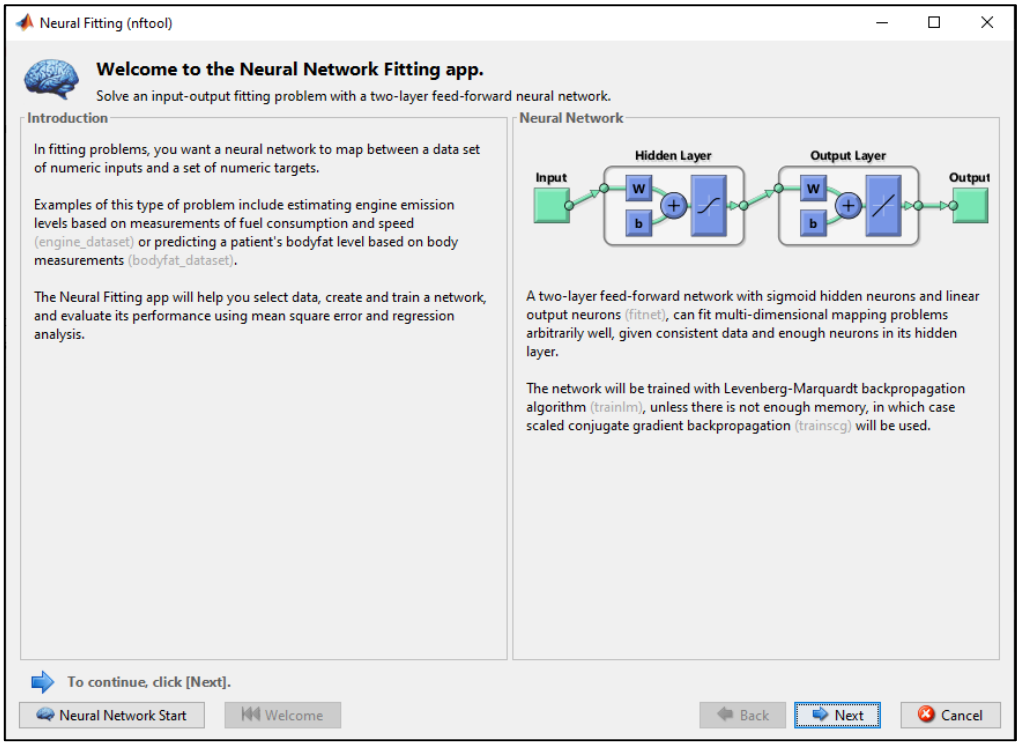

Figure (III.10): Setting Up the Neural Network Fitting Tool

This figure introduces the Neural Network Fitting app, explaining its purpose, which is to solve an input-output fitting problem using a two-layer feed-forward neural network.

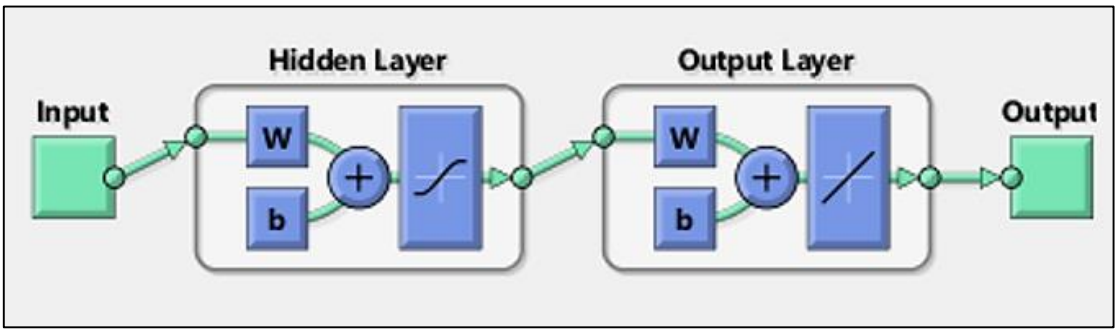

Figure (III.11): Neural Network Structure

The diagram shows the structure of the neural network, which includes an input layer, hidden layers, and an output layer.

Training Algorithm: It mentions that the network will be trained using the Levenberg-Marquardt backpropagation algorithm (trainlm).

3. Select Data :

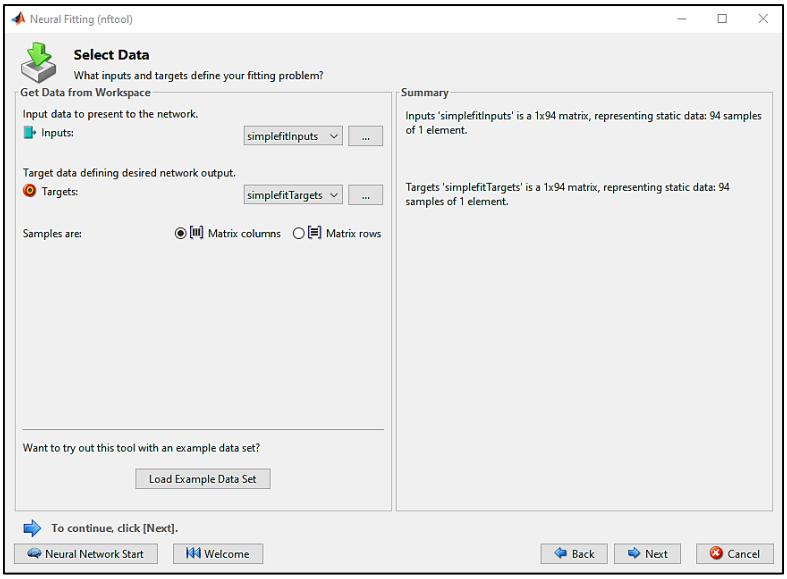

Figure (III.12): Select Data

Inputs and Targets : This figure allows you to select the input and target data from the MATLAB workspace.

Data Summary : The summary on the right shows the dimensions of the selected data. Here, 'simplefitInputs' and 'simplefitTargets' are used as example datasets, with 94 samples each.

4. Import Data :

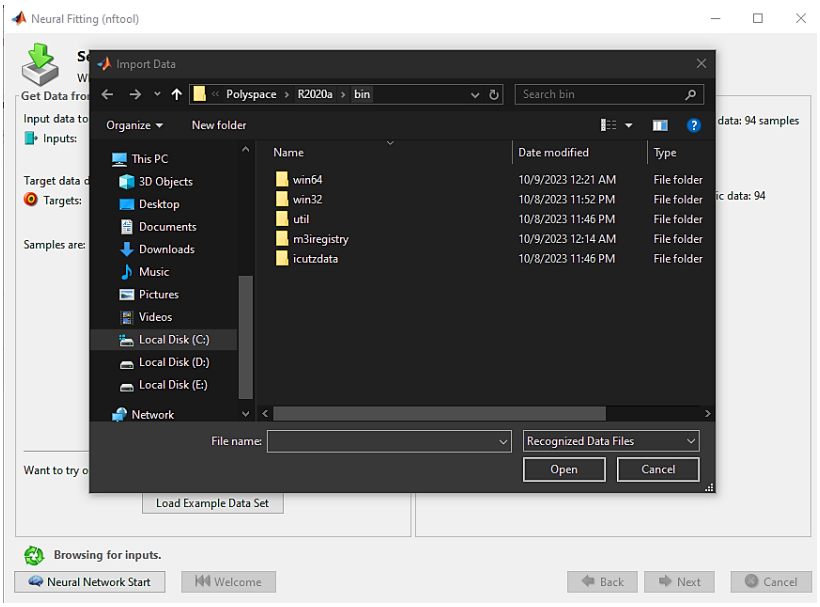

Figure (III.13): Import Data

Data Import: If the data is not already in the workspace, this figure allows you to browse and import data files from your computer. This ensures that the input and target datasets are correctly loaded into MATLAB for network training.

5. Validation and Test Data :

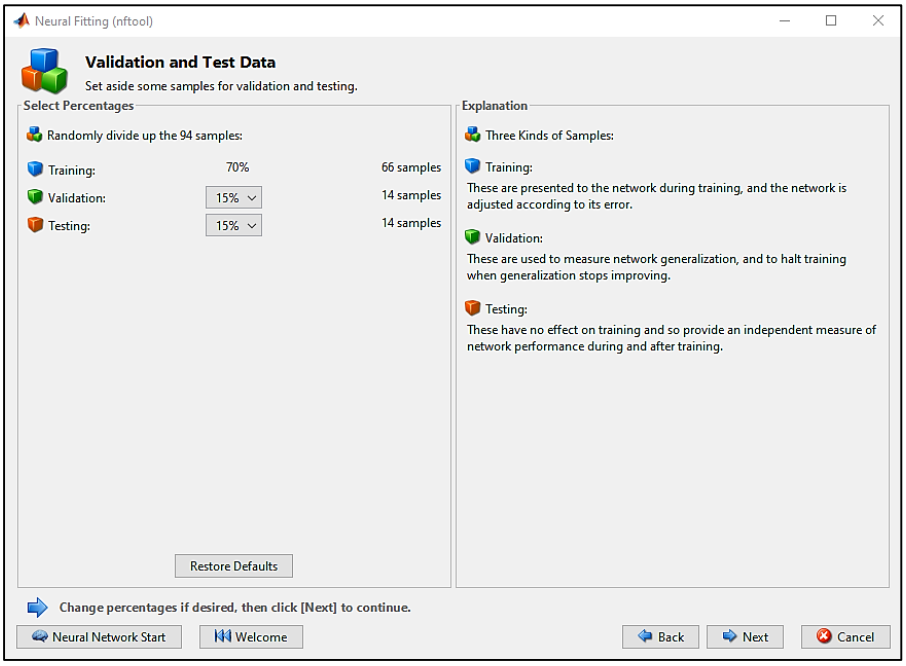

Figure (III.14): Validation and Test Data

Data Division: This figure divides the dataset into training, validation, and testing subsets. The default division is 70% training, 15% validation, and 15% testing.

Explanation: Training data is used to train the network, validation data is used to prevent overfitting by stopping training when performance worsens, and testing data is used to independently assess the network's performance.

6. Network Architecture :

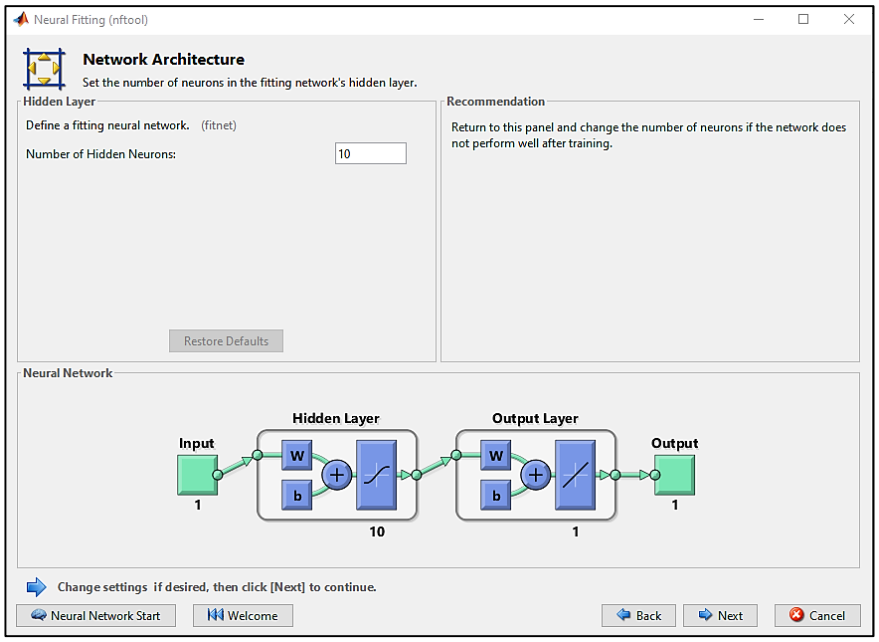

Figure (III.15): Network Architecture

Hidden Layer Configuration: This figure allows you to set the number of neurons in the hidden layer(s). In this example, there are 10 neurons in the hidden layer[21].

Network Diagram: The diagram below visually represents the structure of the network with the specified number of hidden neurons.

7. Network Training :

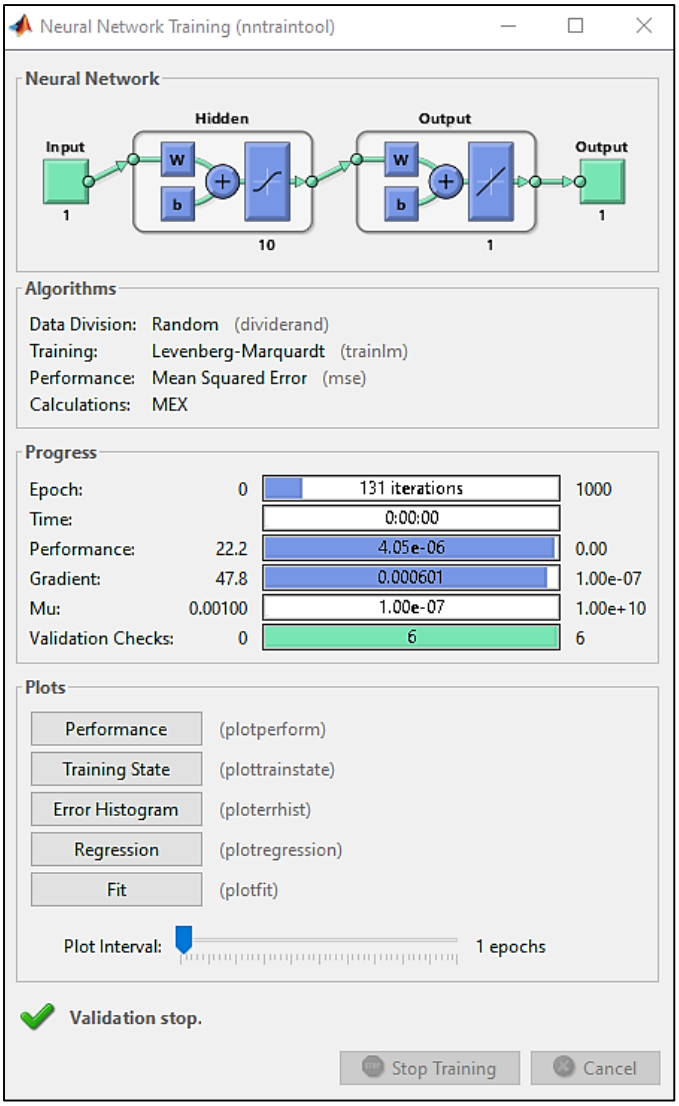

Figure (III.16): Network Training

Training Process: This figure shows the progress of the network training, including the number of epochs, performance, gradient, and validation checks.

Performance Plots: Various plots are available to monitor the training process, including performance, training state, error histogram, and regression plots.

Stop Training: You can manually stop the training process if needed[22].

8. Train Network :

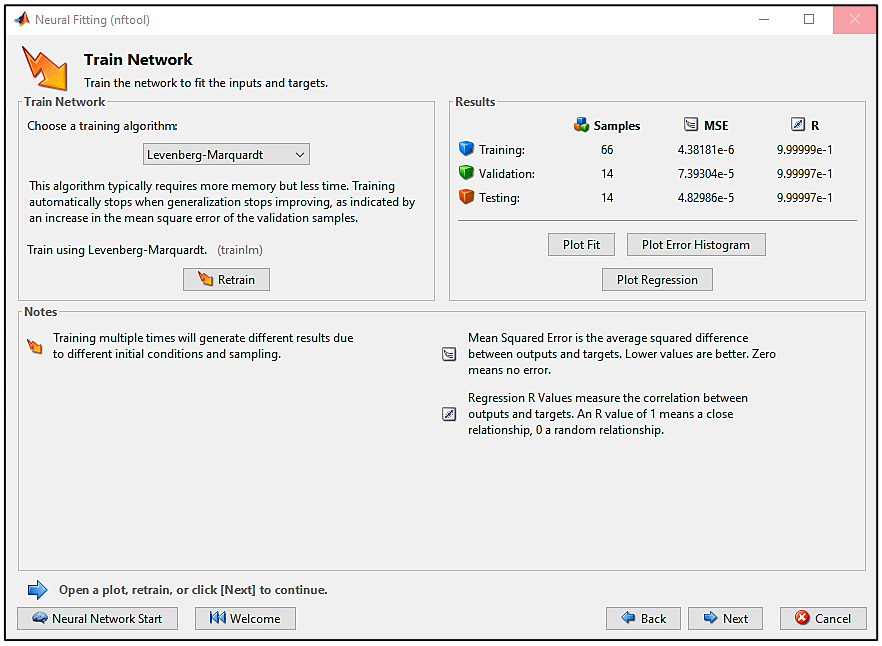

Figure (III.17): Train Network

Training Results: After training, this figure shows the results, including the mean squared error (MSE) for the training, validation, and testing datasets.

Regression Plot: This plot shows the correlation between the network outputs and the targets. A high R-value close to 1 indicates a good fit.

Error Histogram: This plot shows the distribution of errors between the network outputs and the targets[22].

III.6. Conclusion :

In this chapter, we have begun the most important and most delicate part of this study. This involves presenting the principle of searching for the maximum power point while giving the different classifications of MPPT commands. We have detailed the different MPPT methods encountered most often in literature. The existence of several types of MPPT commands shows that this area of research is constantly evolving and that it is difficult to find one or more universal solutions.

Chapter IV

Simulation Results

IV.1. Introduction :

In this chapter, we delve into the performance evaluation and comparison of three widely recognized Maximum Power Point Tracking (MPPT) algorithms Perturb and Observe (P&O), Incremental Conductance (INC), and Artificial Neural Network (ANN). These algorithms play a crucial role in optimizing the power output of photovoltaic (PV) systems by continuously adjusting the operating point to ensure maximum energy extraction from solar panels. By accurately tracking the maximum power point, these algorithms help in maximizing the efficiency and effectiveness of PV systems, which is essential for improving the overall performance and energy yield. The P&O algorithm relies on periodic perturbations and observations to find the optimal point, whereas the INC algorithm uses the incremental conductance method for finer adjustments. The ANN algorithm, on the other hand, leverages artificial intelligence to predict and track the maximum power point with high precision. Our comprehensive analysis aims to highlight the strengths and weaknesses of each algorithm, providing valuable insights into their suitability for different operating conditions.

IV.2. Parameters of System Simulation :

The following characteristics of panel and the parameters of boost converter that are used in our system simulation, are shown in the figure and table below:

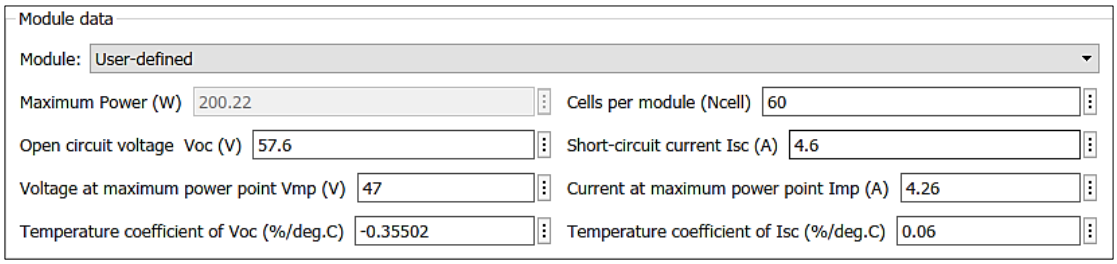

Figure (IV.1): Characteristics of Panel

Boost Converter	Value
Capacitor 1	200 µF
Inductor	3.5 mH
Capacitor 2	100 µF
Resistive Load	300 Ω

Table (IV.1): Parameters of Boost Converter

IV.3. Simulation Results :

IV.3.1. P&O Algorithm :

In this simulation, we used the Perturb and Observe (P&O) algorithm to obtain results for power, voltage, and current. Figure (IV.2) represents the general system simulation, showcasing the overall setup and performance of the P&O -based MPPT system. The figure illustrates the integration of PV panels with the P&O -based MPPT controller, which adjusts the duty cycle to optimize power extraction.

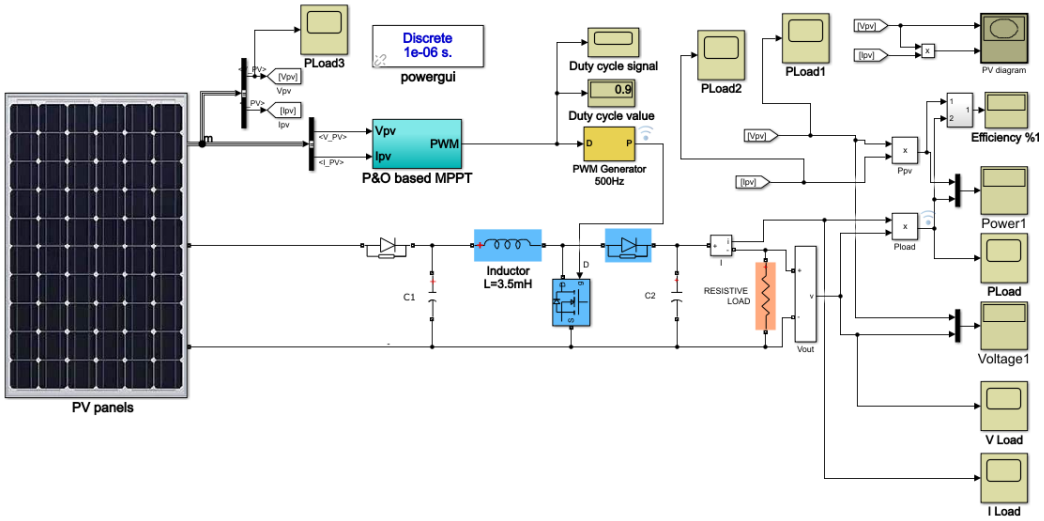

Figure (IV.2): Schema of System Simulation With P&O

a) Constant Irradiance (1000 W/m^2) :

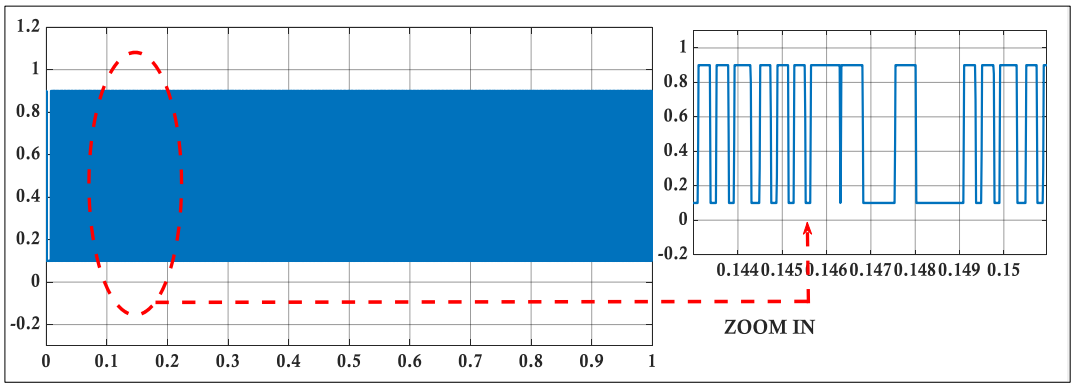

Figure (IV.3): Duty Cycle Simulation Result

The Figure (IV.3) demonstrates the MPPT system's duty cycle behavior, with the main plot showing overall stability and the zoomed-in view revealing critical fluctuations for precise MPPT operation.

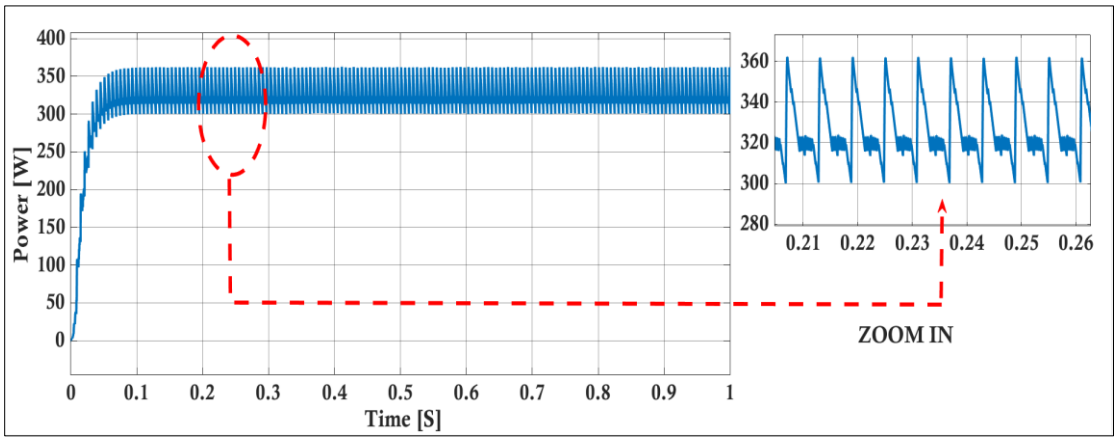

Figure (IV.4): Power Simulation Result

The Figure (IV.4) illustrates the power response of an MPPT system using the P&O algorithm. The main plot shows a rapid increase in power followed by stabilization around 350W. The zoomed-in view highlights the oscillatory nature of the power output, characteristic of the P&O algorithm as it continuously perturbs to track the maximum power point. These oscillations are a trade-off for maintaining optimal power extraction and are crucial for understanding the efficiency and performance of the MPPT system.

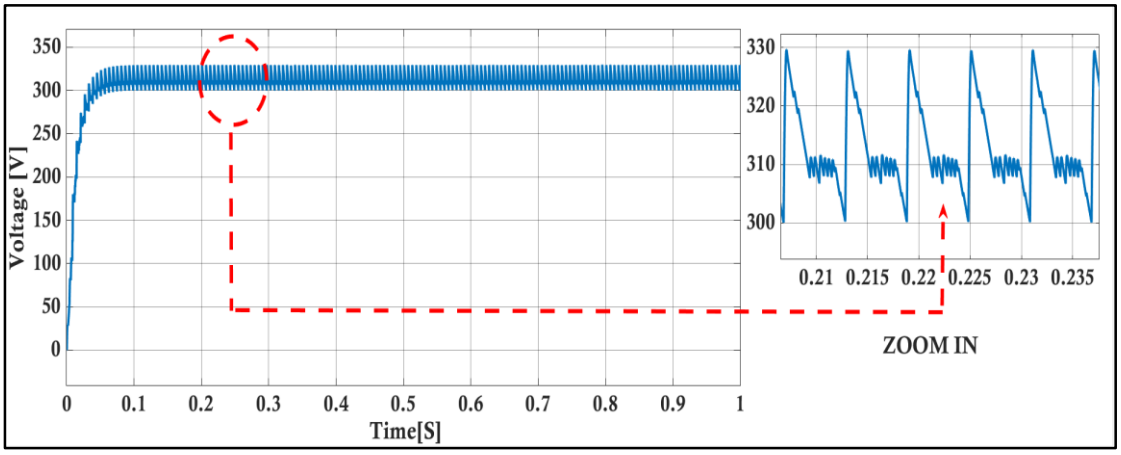

Figure (IV.5): Voltage Simulation Result

The Figure (IV.5) illustrates the voltage response of an MPPT system using the P&O algorithm. The main plot shows a rapid increase in voltage, stabilizing around 320V. The zoomed-in view highlights the oscillatory nature of the voltage output.

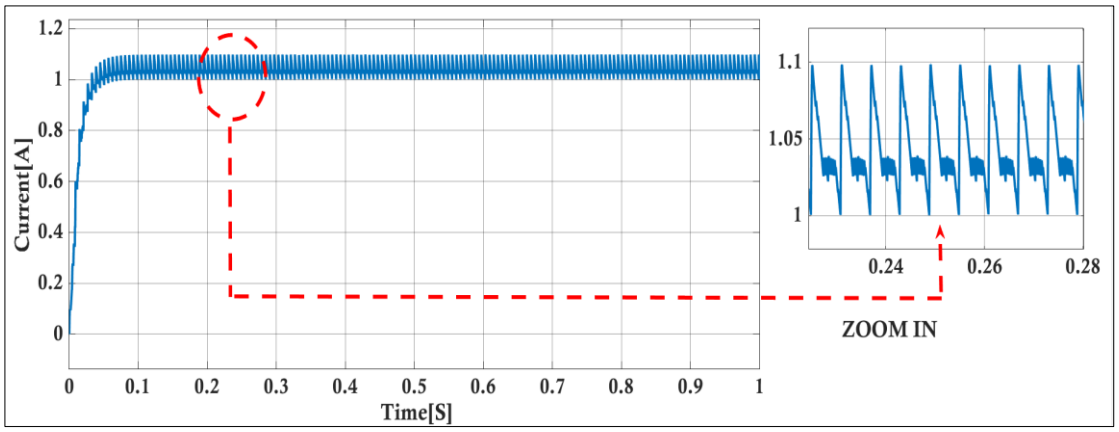

Figure (IV.6): Current Simulation Result

The Figure (IV.6) illustrates the current response of an MPPT system using the P&O algorithm. the main plot shows the rapid transient response leading to stabilization at approximately 1.05A, indicative of the system reaching its maximum power point. The zoomed-in view provides a closer look at the inherent oscillations around this steady-state value

b) Variable Irradiances (1000, 800, 600, 400 W/m^2) :

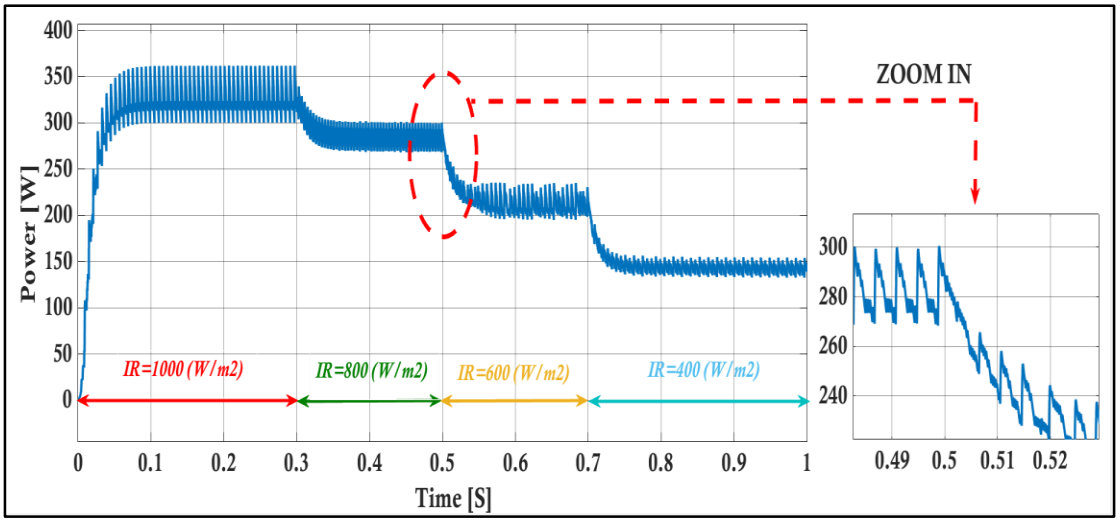

Figure (IV.7): Power Simulation Result

The Figure (IV.7) provides a comprehensive view of the MPPT system's power output behavior under varying irradiance levels. The main plot demonstrates the system's ability to track the maximum power point across different irradiances, with power stabilizing at approximately 350 W, 300 W, 250 W, and 200 W for IR levels of 1000 W/m², 800 W/m², 600 W/m², and 400 W/m², respectively. The red dashed ellipse and zoomed-in view emphasize the system's transient response to a sudden drop in

irradiance, showcasing the characteristic oscillations as the P&O algorithm adjusts to the new maximum power point. This detailed analysis underscores the efficiency and adaptability of the MPPT system in real-time solar energy applications

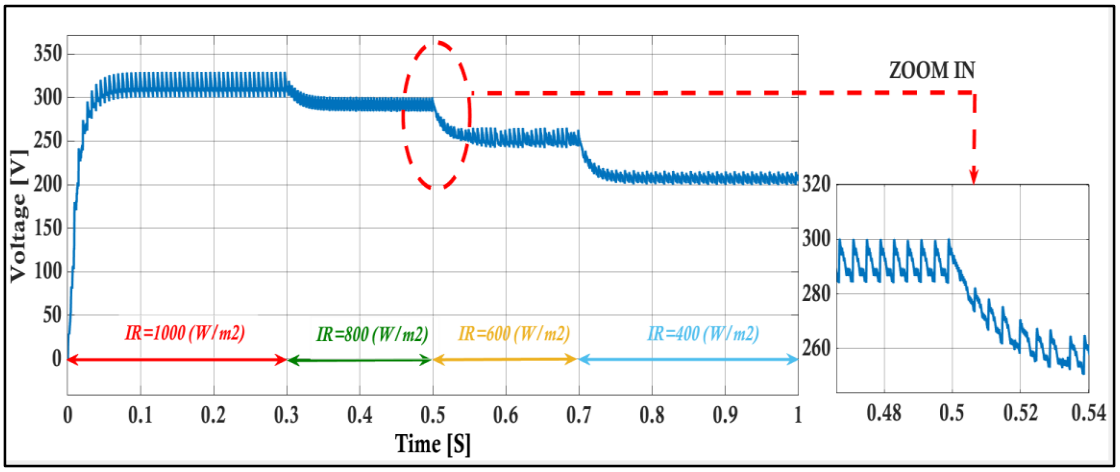

Figure (IV.8): Voltage Simulation Result

The Figure (IV.8) demonstrates how the voltage of an MPPT system using the P&O algorithm adjusts to varying irradiance levels. The main plot shows the system's quick voltage stabilization at around 320V, followed by stepwise decreases as the irradiance drops. The zoomed-in view provides a detailed look at the transient fluctuations, illustrating the algorithm's continuous adjustments to maintain optimal performance.

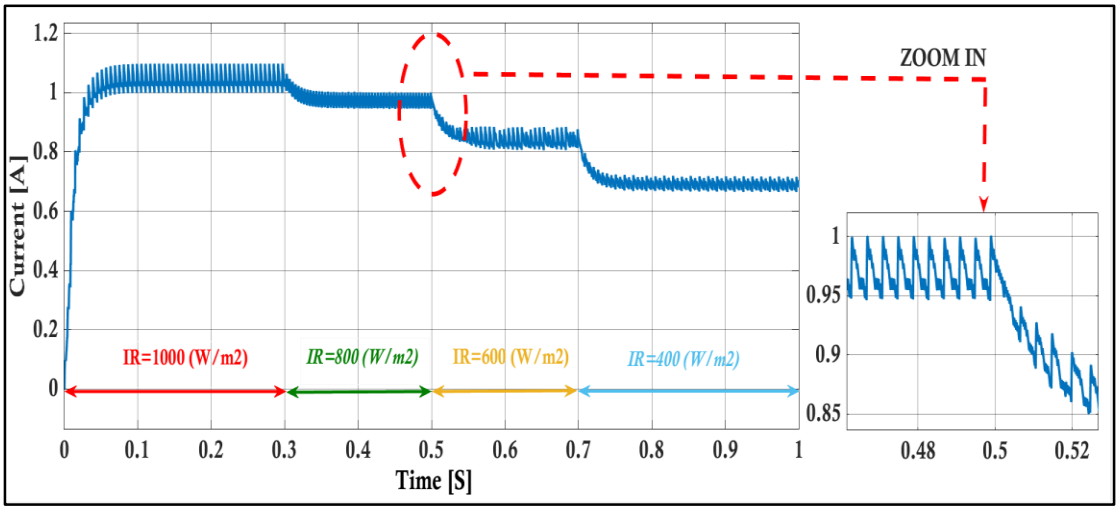

Figure (IV.9): Current Simulation Result

The Figure (IV.9) demonstrates how the MPPT system's current output, managed by the P&O algorithm, adjusts under varying irradiance levels. The main plot shows the current stabilizing around 1A and decreasing in steps as irradiance diminishes. The zoomed-in view captures the transient response during an irradiance change.

IV.3.2. Incremental Conductance :

In this simulation, we used the Incremental Conductance (INC) algorithm to obtain results for power, voltage, and current. Figure (IV.10) represents the general system simulation, showcasing the overall setup and performance of the INC-based MPPT system. The figure illustrates the integration of PV panels with the INC-based MPPT controller, which adjusts the duty cycle to optimize power extraction.

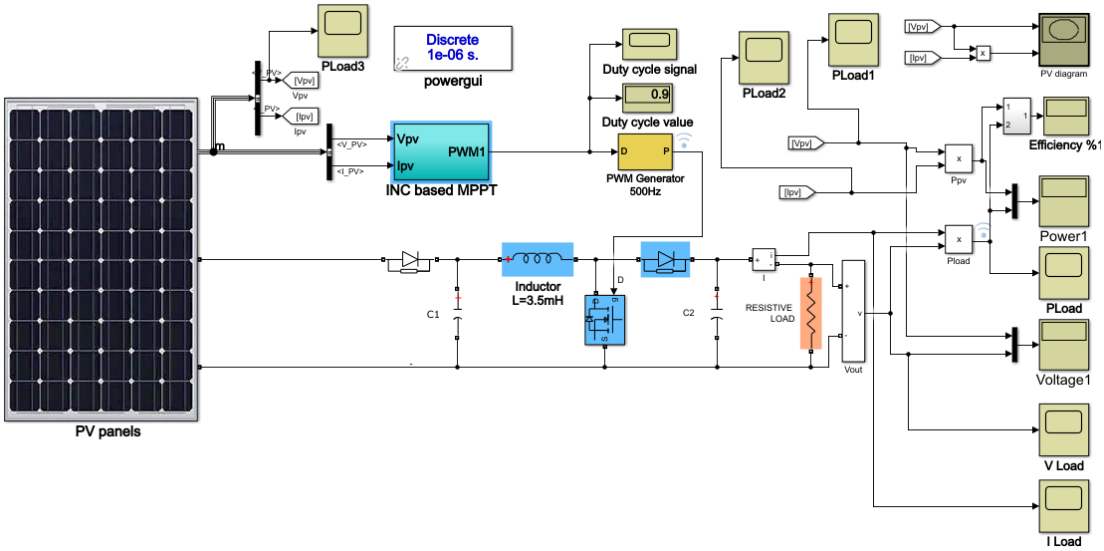

Figure (IV.10): Schema of System Simulation With INC

a) Constant Irradiance (1000 W/m^2) :

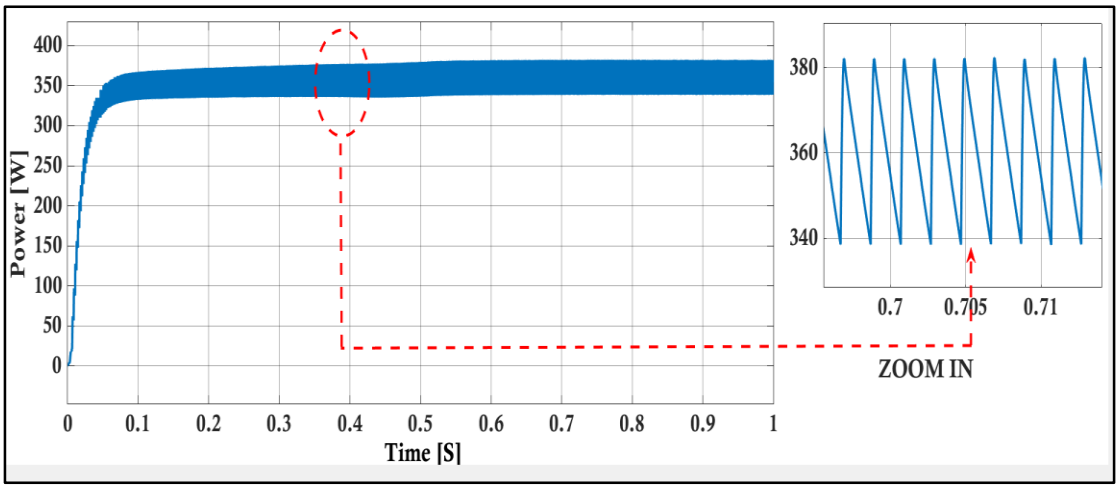

Figure (IV.11): Power Simulation Result

The Figure (IV.11) demonstrates the power stabilization behavior of an MPPT system managed by the Incremental Conductance algorithm. The main plot shows a rapid rise and stabilization of power at approximately 370W, reflecting the system's

efficiency. The zoomed-in view highlights periodic fluctuations, illustrating the algorithm's continuous adjustments to maintain optimal power output. This analysis underscores the Incremental Conductance algorithm's capability to dynamically track the maximum power point with precision.

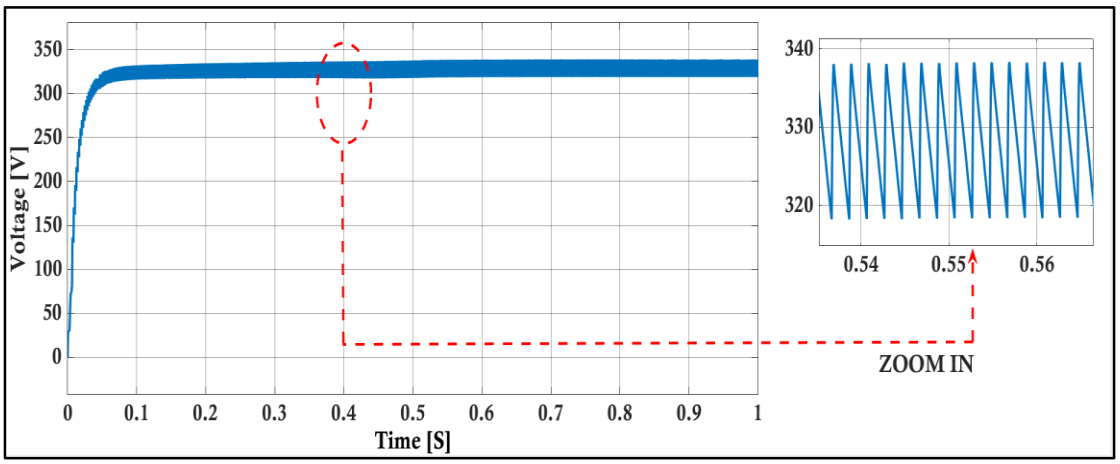

Figure (IV.12): Voltage Simulation Result

The Figure (IV.12) demonstrates the voltage response of an Incremental Conductance-based MPPT system. The main plot shows the voltage stabilizing around 330V, while the zoomed-in view captures small fluctuations.

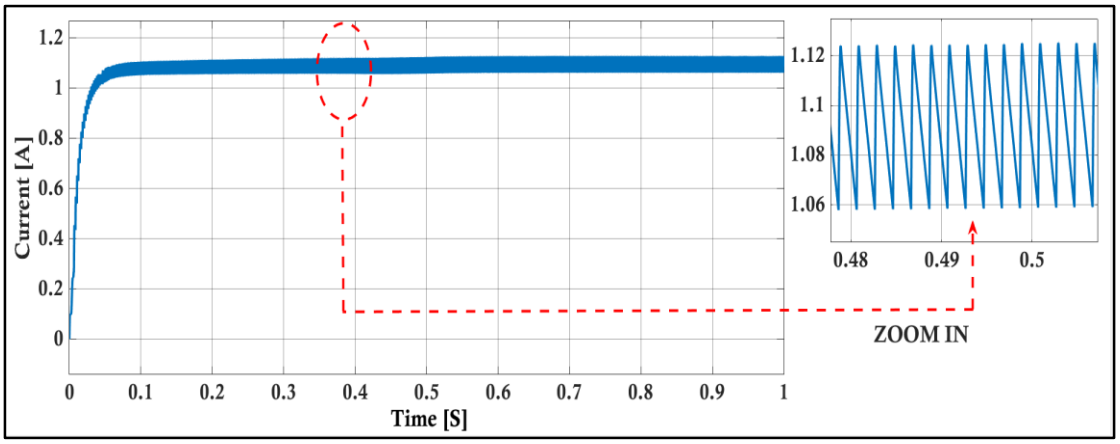

Figure (IV.13): Current Simulation Result

The Figure (IV.13) demonstrates the current stabilization behavior of an MPPT system managed by the Incremental Conductance algorithm. The main plot shows the current quickly rising and stabilizing around 1.1A, indicating the system's efficiency in reaching the maximum power point. The zoomed-in view highlights small fluctuations in the current.

b) Variable Irradiances (1000, 800, 600, 400 W/m^2) :

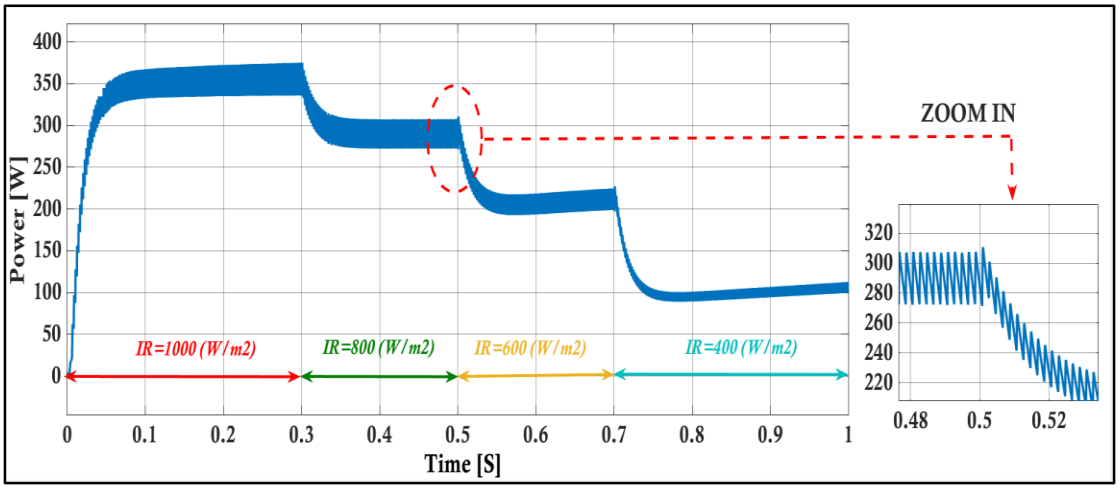

Figure (IV.14): Power Simulation Result

The Figure (IV.14) demonstrates the power response of an MPPT system using the Incremental Conductance algorithm under varying irradiance conditions. The main plot shows the power stabilizing around 350W initially, with stepwise decreases as the irradiance drops. The zoomed-in view captures the transient fluctuations during an irradiance change.

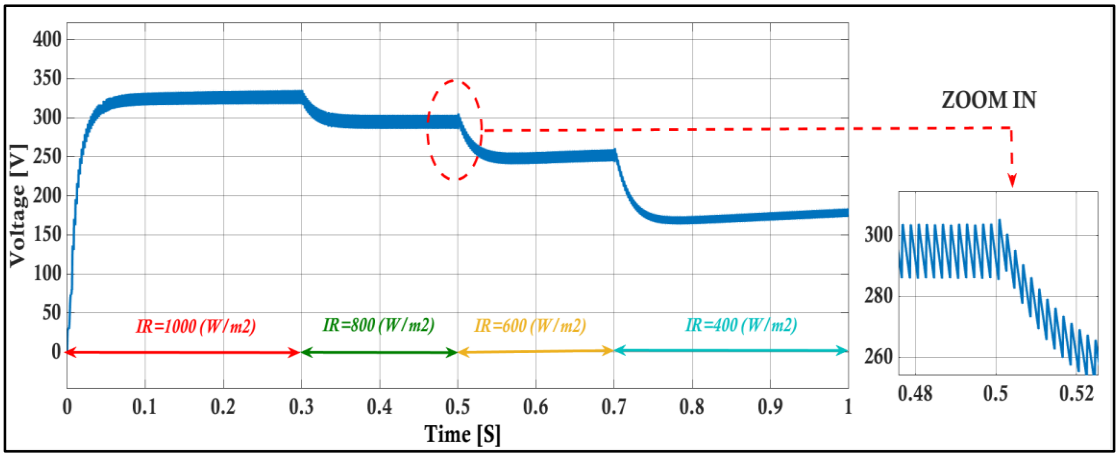

Figure (IV.15): Voltage Simulation Result

The Figure (IV.15) demonstrates the voltage response of an Incremental Conductance-based MPPT system to varying irradiance levels. The main plot shows a rapid rise and stabilization around 330V, with stepwise decreases as irradiance drops. The zoomed-in view highlights transient fluctuations,

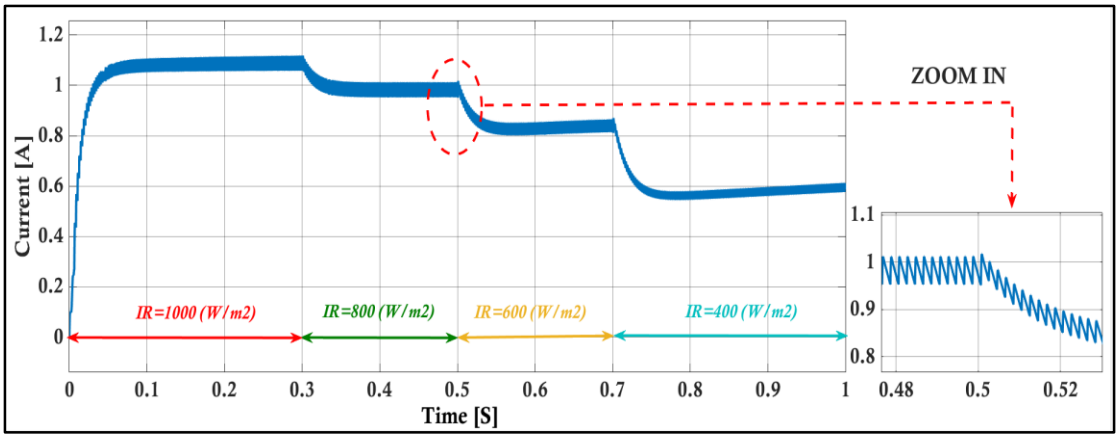

Figure (IV.16): Current Simulation Result

The Figure (IV.16) demonstrates the current response of an MPPT system using the Incremental Conductance algorithm under varying irradiance conditions. The main plot shows the current stabilizing around 1.1A initially, with stepwise decreases as the irradiance drops. The zoomed-in view captures transient fluctuations during an irradiance change.

IV.3.3. Artificial Neural Network (ANN) :

In this simulation, we used the Artificial Neural Network (ANN) algorithm to obtain results for power, voltage, and current. Figure (IV.17) represents the general system simulation, showcasing the overall setup and performance of the ANN-based MPPT system. The figure illustrates the integration of PV panels with the ANN-based MPPT controller, which adjusts the duty cycle to optimize power extraction.

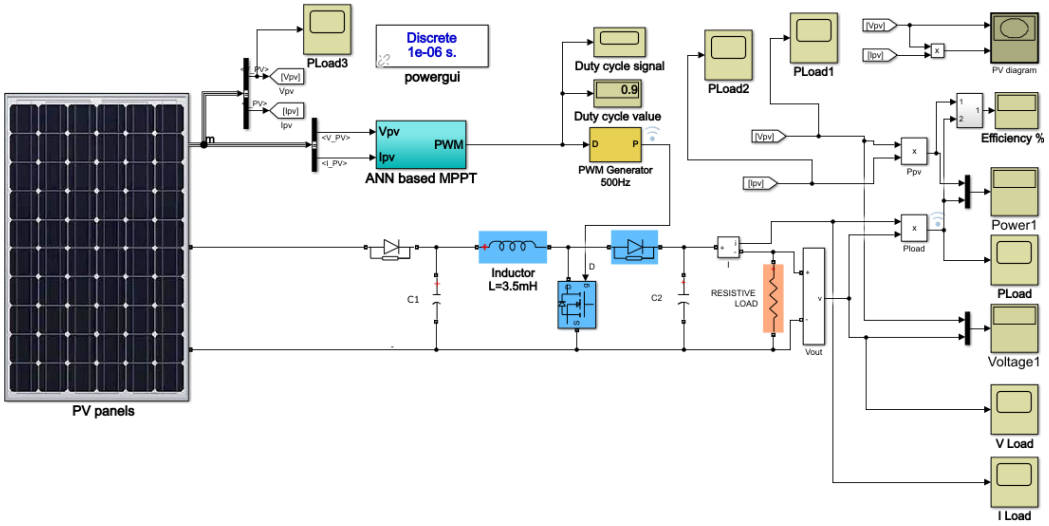

Figure (IV.17): Schema of System Simulation With ANN

a) Constant Irradiance (1000 W/m^2) :

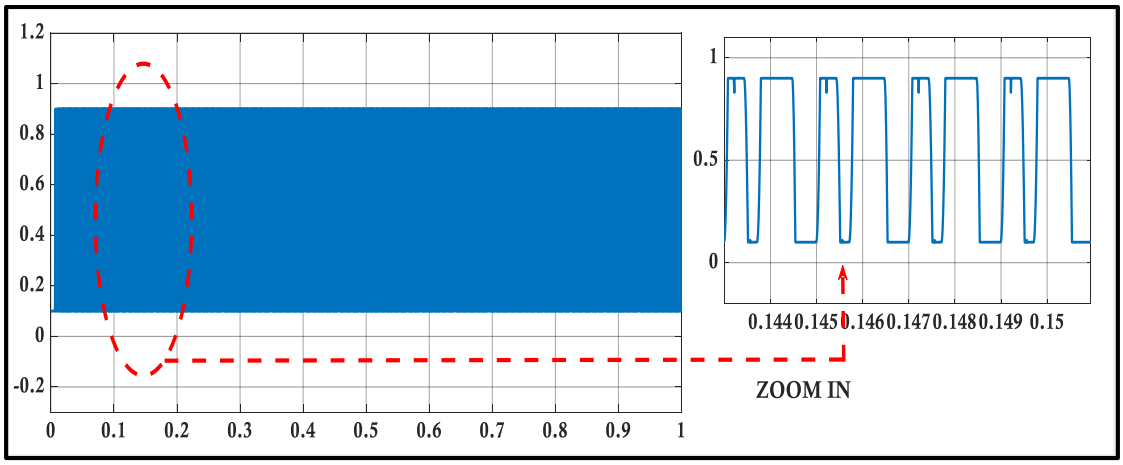

Figure (IV.18): Duty Cycle Simulation Result

The Figure (IV.18) demonstrates the stability and fine-tuning of the duty cycle by an ANN-based MPPT system. The main plot shows a stable duty cycle near 1, while the zoomed-in view reveals periodic adjustments, indicating the ANN's responsiveness to optimize performance.

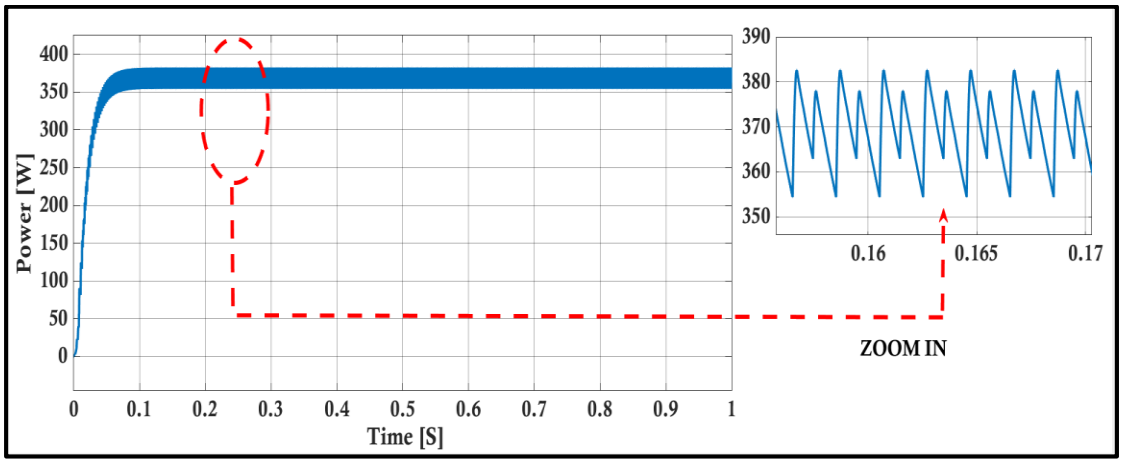

Figure (IV.19): Power Simulation Result

The Figure (IV.19) demonstrates the power stabilization behavior of an MPPT system managed by an ANN algorithm. The main plot indicates a rapid rise and stabilization of power at approximately 380W, reflecting the system's efficiency. The zoomed-in view highlights periodic fluctuations, illustrating the ANN's ongoing adjustments to maintain optimal power output. This analysis underscores the ANN algorithm's capability to dynamically track the maximum power point with precision.

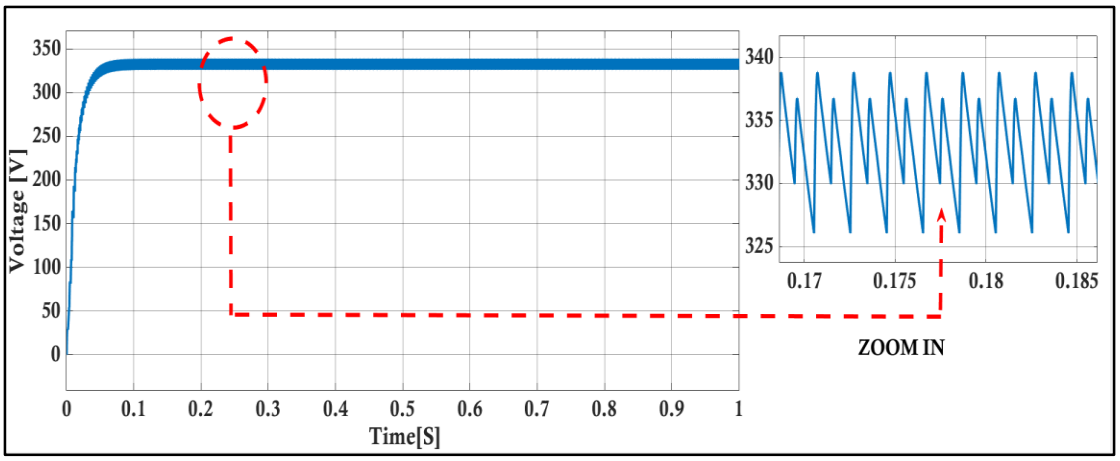

Figure (IV.20): Voltage Simulation Result

The Figure (IV.20) illustrates the voltage behavior of an ANN-based MPPT system. The main plot shows a quick rise and stabilization around 335V, while the zoomed-in view captures small fluctuations.

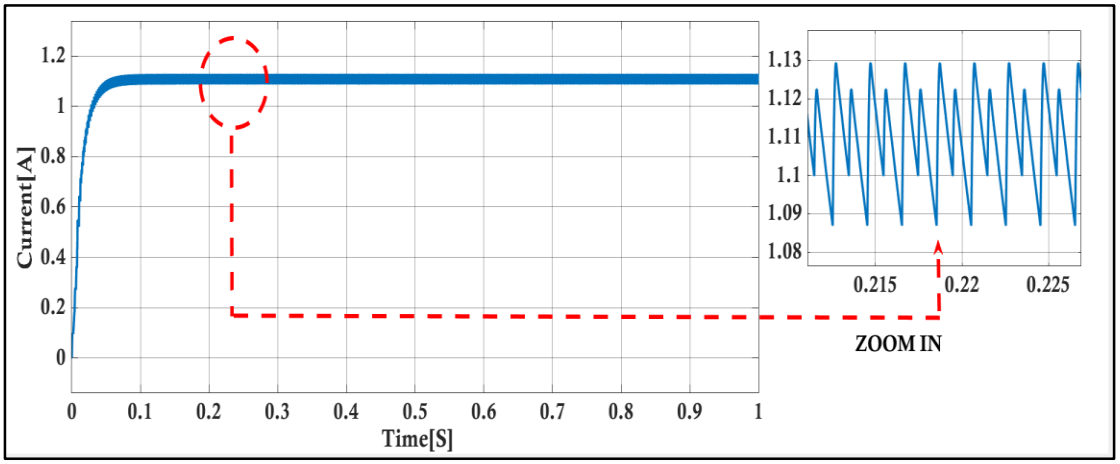

Figure (IV.21): Current Simulation Result

The Figure (IV.21) shows the current stabilization of an ANN-based MPPT system. The main plot displays a rapid rise in current, stabilizing around 1.1A. The zoomed-in view highlights small fluctuations.

b) Variable Irradiances (1000, 800, 600, 400 W/m^2) :

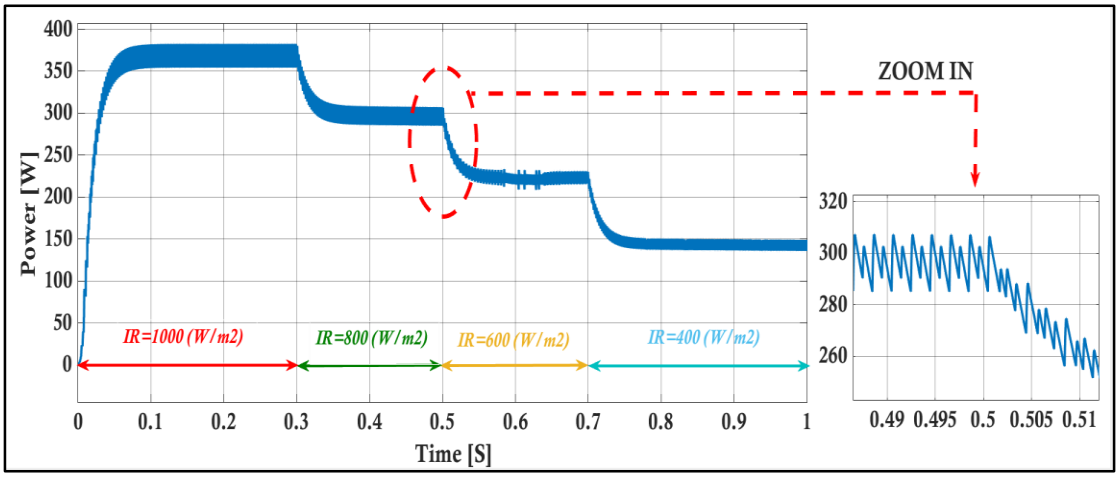

Figure (IV.22): Power Simulation Result

The Figure (IV.22) demonstrates how the ANN-based MPPT system adjusts its power output under varying irradiance conditions. The main plot shows the power stabilizing at approximately 350W initially, with stepwise decreases as the irradiance drops. The zoomed-in view captures the transient fluctuations during an irradiance change.

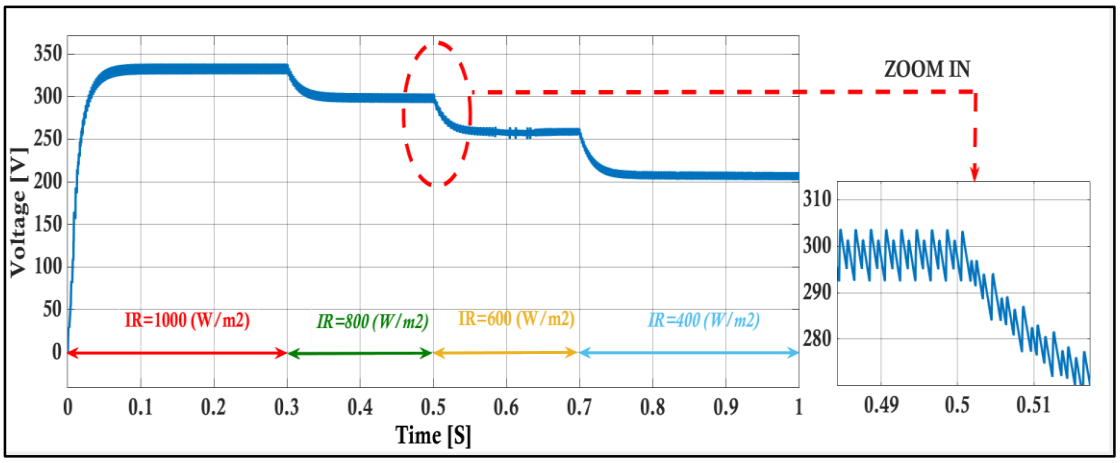

Figure (IV.23): Voltage Simulation Result

The Figure (IV.23) illustrates the ANN-based MPPT system's voltage response to varying irradiance. The main plot shows the voltage stabilizing around 330V and stepping down with decreasing irradiance. The zoomed-in view highlights transient fluctuations This demonstrates the algorithm's capability to dynamically adjust to real-time changes in solar irradiance, ensuring efficient performance.

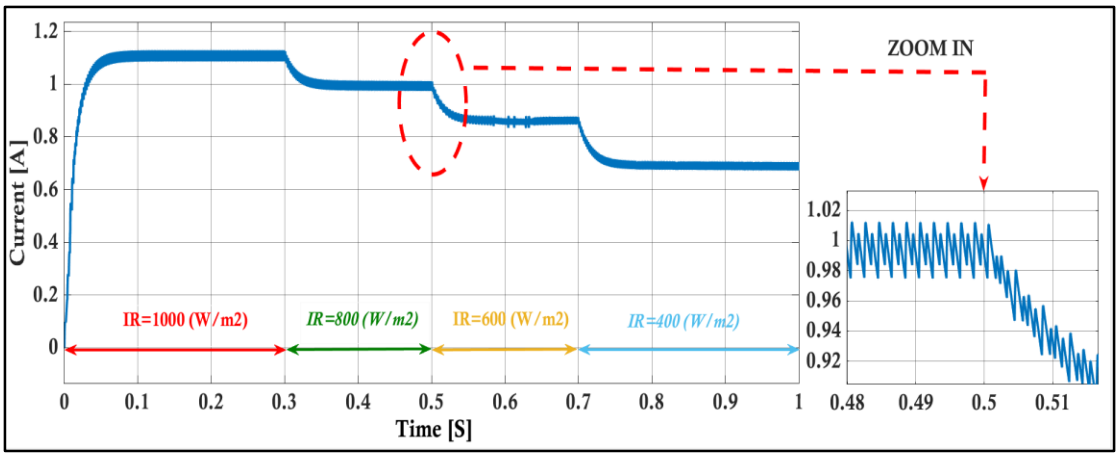

Figure (IV.24): Current Simulation Result

The Figure (IV.24) demonstrates the current response of an ANN-based MPPT system under varying irradiance conditions. The main plot shows the current stabilizing around 1.1A initially, with stepwise decreases as the irradiance drops. The zoomed-in view captures transient fluctuations during an irradiance change.

IV.4. Comparison and Analysis Between (P&O, INC, ANN) :

IV.4.1. Constant Irradiance (1000 W/m^2) :

The following figures compare the current and voltage outputs of three MPPT algorithms: Incremental Conductance (INC), Perturb and Observe (P&O), and Artificial Neural Network (ANN).

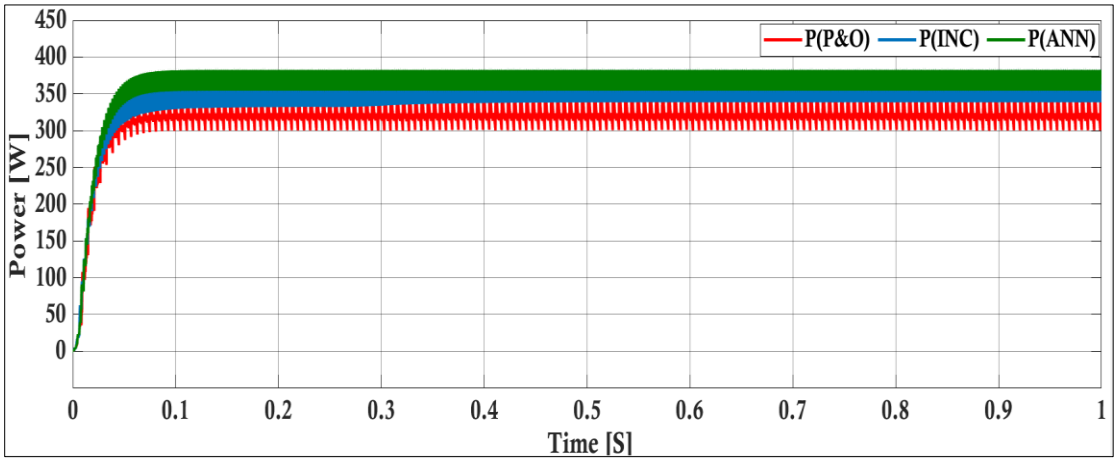

Figure (IV.25): Power Simulation Result

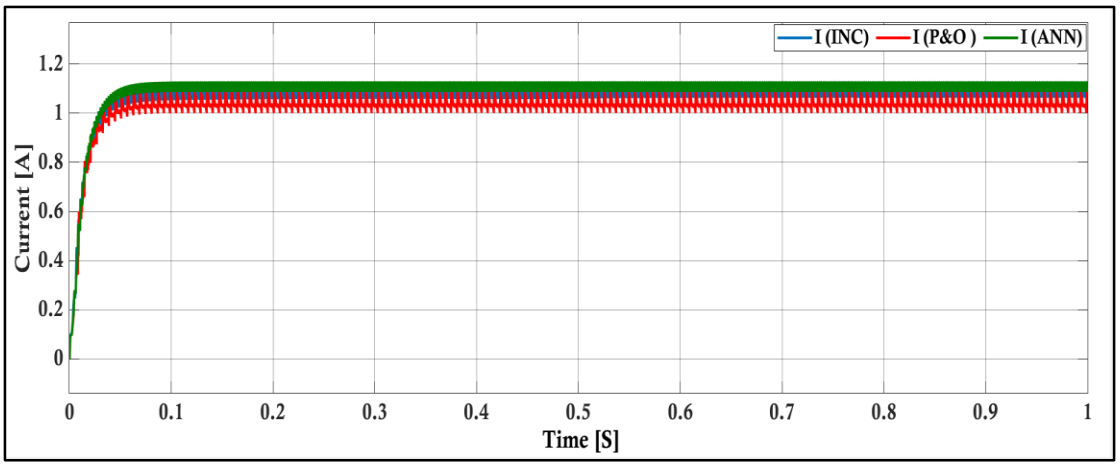

Figure (IV.26): Current Simulation Result

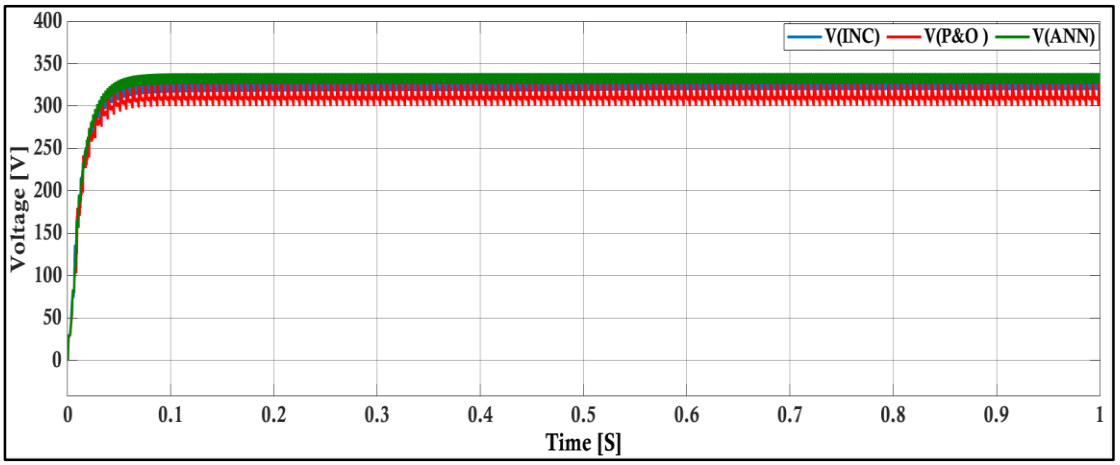

Figure (IV.27): Voltage Simulation Result

IV.4.1.1. Comparison :

- **Incremental Conductance (INC)**: This algorithm shows rapid stabilization in both current and voltage with minimal fluctuations, indicating efficient and stable performance.
- **Perturb and Observe (P&O)**: While it also achieves rapid stabilization, it exhibits more fluctuations in both current and voltage, indicating less stability compared to the other two algorithms.
- **Artificial Neural Network (ANN)**: This algorithm achieves stabilization with minimal fluctuations, similar to INC, suggesting efficient and stable performance.

IV.4.1.2. Analysis:

- **Best Performance**: Both INC and ANN show better performance with minimal fluctuations in current and voltage, suggesting they are more stable and efficient in tracking the maximum power point compared to P&O.
- **Slight Edge**: ANN might have a slight edge over INC due to its adaptive nature and potential for better optimization in varying conditions.

Therefore, based on these figures, the Artificial Neural Network (ANN) algorithm appears to be the best option for MPPT, offering efficient stabilization with minimal fluctuations, closely followed by the Incremental Conductance (INC) algorithm.

IV.4.2. Variable Irradiances (1000, 800, 600, 400 W/m^2) :

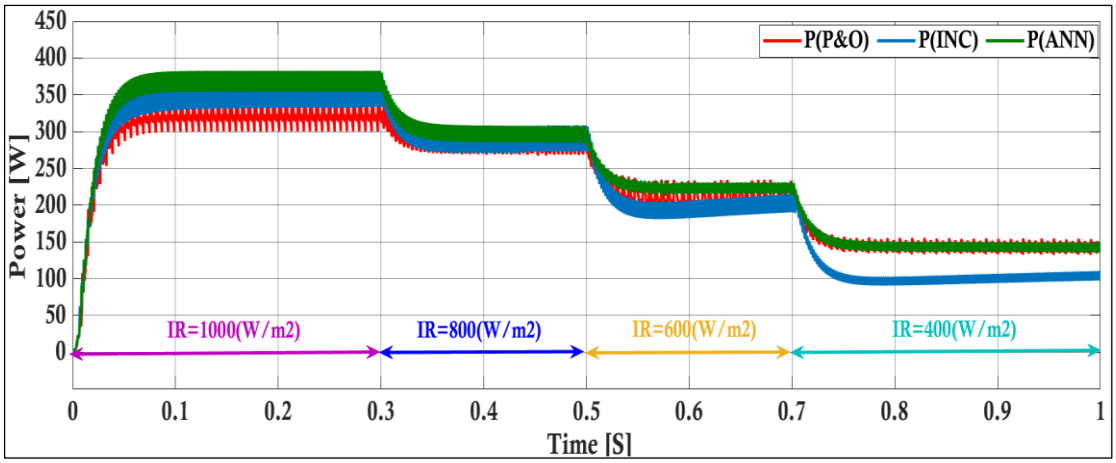

Figure (IV.28): Power Simulation Result

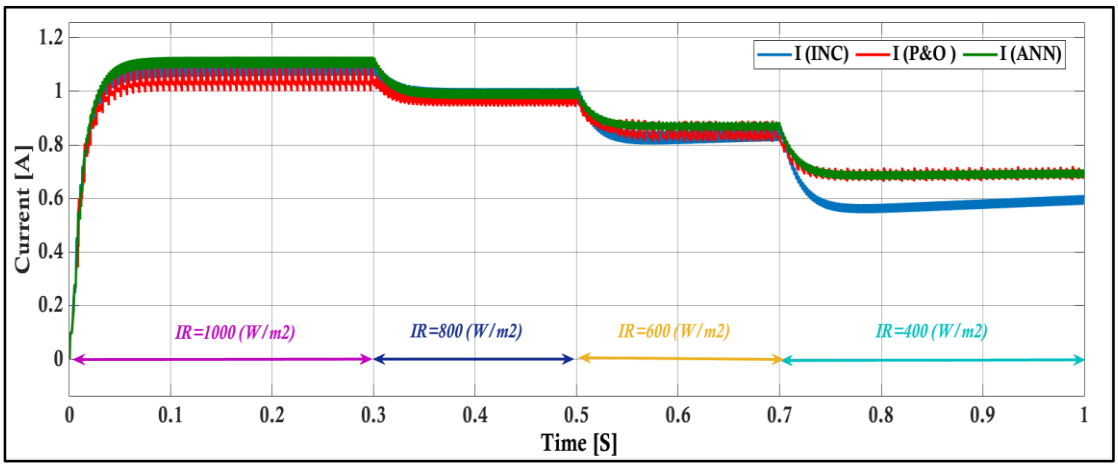

Figure (IV.29): Current Simulation Result

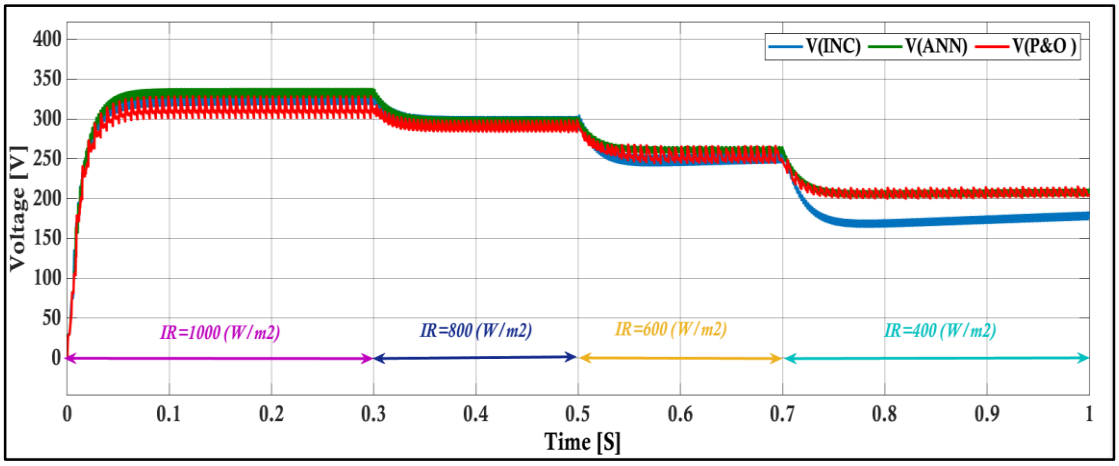

Figure (IV.30): Voltage Simulation Result

IV.4.2.1. Comparison :

- **Incremental Conductance (INC)** : This algorithm shows rapid stabilization but exhibits more fluctuations and deviations during irradiance changes, indicating less stability compared to the other two algorithms.
- **Perturb and Observe (P&O)** : This algorithm shows noticeable fluctuations and is less stable during transitions between irradiance levels.
- **Artificial Neural Network (ANN)** : This algorithm exhibits the least fluctuations and the smoothest transitions during changes in irradiance, indicating the highest stability and efficiency.

IV.4.2.2. Analysis :

- **Best Performance** : The Artificial Neural Network (ANN) algorithm demonstrates the best performance with minimal fluctuations and smooth transitions during varying irradiance levels, indicating superior stability and efficiency.
- **Slight Edge** : The ANN algorithm has a slight edge over the Incremental Conductance (INC) and Perturb and Observe (P&O) algorithms due to its adaptive nature and better optimization in dynamic conditions.

Based on these figures, the Artificial Neural Network (ANN) algorithm appears to be the best option for MPPT, offering the most stable and efficient performance under varying irradiance conditions.

IV.5. Comparison of efficiency between algorithms (P&O, INC, ANN) :

IV.5.1. Constant Irradiance (1000 W/m^2) :

Algorithm	Efficiency
Perturb and Observe (P&O)	94.72%
Incremental Conductance (INC)	95.58%
Artificial Neural Network (ANN)	96.63%

Table (IV.2): Table of Efficiency

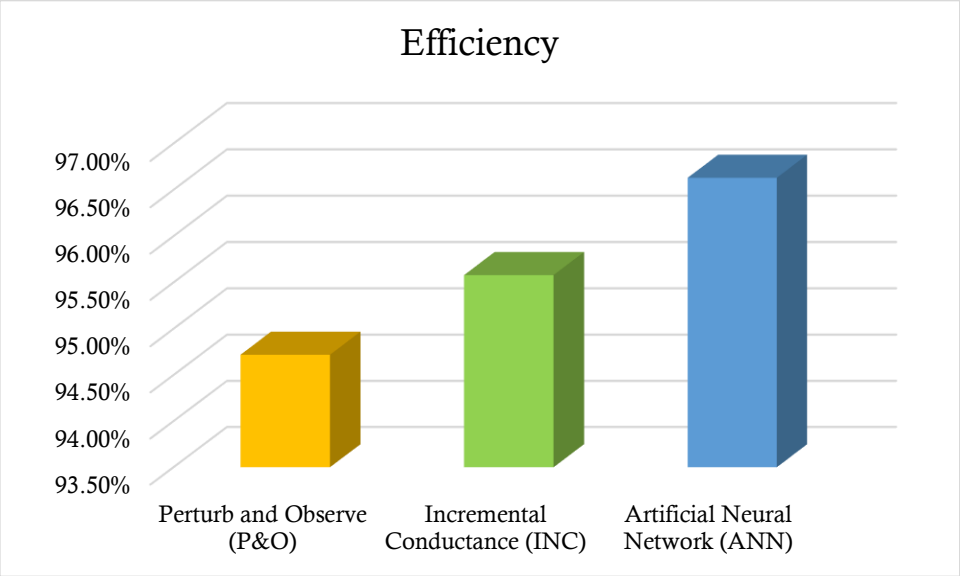

Figure (IV.31): Chart of Efficiency

Under constant irradiance of 1000 W/m², the Artificial Neural Network (ANN) algorithm demonstrates the highest efficiency, around 97%. The Incremental Conductance (INC) algorithm follows with an efficiency of about 96%, while the Perturb and Observe (P&O) algorithm has the lowest efficiency at approximately 95%. This indicates that the ANN algorithm is the most effective in optimizing power output under stable irradiance conditions, outperforming both the INC and P&O algorithms.

IV.5.2. Variable Irradiances (1000, 800, 600, 400 W/m^2) :

Algorithm	Efficiency
Perturb and Observe (P&O)	84.84%
Incremental Conductance (INC)	88.04%
Artificial Neural Network (ANN)	95.06%

Table (IV.3): Table of Efficiency

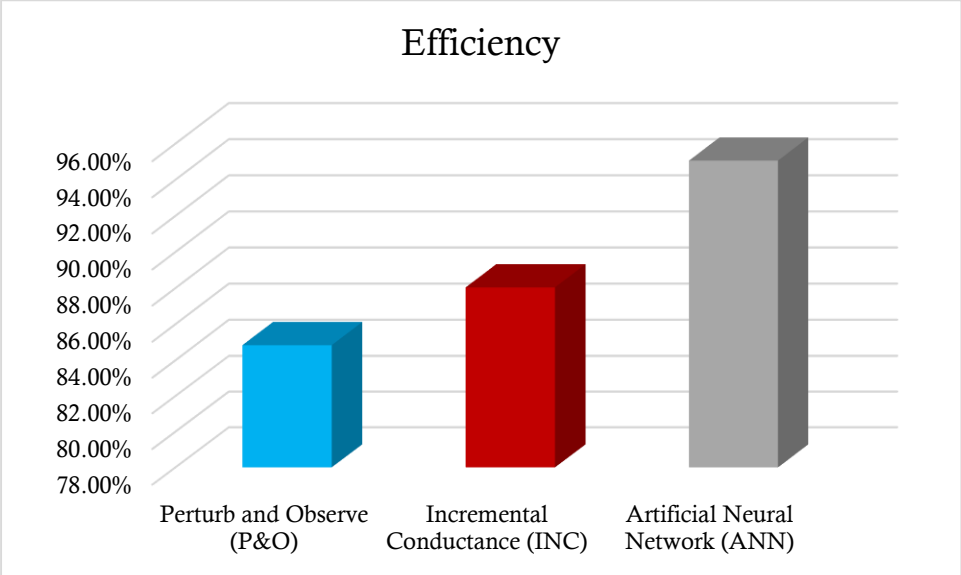

Figure (IV.32): Chart of Efficiency

Under variable irradiance conditions, the Artificial Neural Network (ANN) algorithm demonstrates the highest efficiency, around 95%, indicating its superior ability to adapt to changing light conditions. The Incremental Conductance (INC) algorithm follows with an efficiency of about 89%, showing reasonable performance but less stability compared to ANN. The Perturb and Observe (P&O) algorithm has the lowest efficiency at approximately 86%, reflecting its greater susceptibility to fluctuations under varying irradiance levels. These results highlight the ANN algorithm's effectiveness in optimizing power output in dynamic environments.

IV.6. Conclusion :

The Artificial Neural Network (ANN) algorithm stands out as the most effective and reliable MPPT method in this study. Its superior efficiency, stability, and adaptability under both steady and dynamic irradiance conditions make it the best choice for optimizing photovoltaic system output. The Incremental Conductance (INC) algorithm, while performing better than P&O, still falls short of ANN's advanced capabilities. Despite its common use, the Perturb and Observe (P&O) algorithm is the least effective in this comparison, demonstrating lower efficiency and greater instability. Therefore, for maximizing energy extraction and ensuring reliable performance, the ANN algorithm is the recommended MPPT method.

General Conclusion

General Conclusion

This study began by laying the foundation for understanding solar radiation and photovoltaic energy conversion principles. It explained how solar cells harness the photovoltaic effect to generate electricity from sunlight, and discussed the modeling, characteristics, and factors influencing the efficiency of photovoltaic generators. Different photovoltaic cell types based on silicon crystal structures were also presented. Building upon this, the crucial role of DC-DC converters in power management systems was explored. These converters facilitate efficient voltage conversion through various topologies like buck, boost, and buck-boost, enabling their widespread use across diverse industries.

The concept of Maximum Power Point Tracking (MPPT) was then introduced as a vital technology, particularly for renewable energy systems such as solar power installations. MPPT algorithms optimize energy extraction by continually adjusting the electrical operating point to track the maximum power output of photovoltaic panels.

This naturally led to an in-depth examination of MPPT principles, classifications, and implementation methods. Among the various MPPT algorithms evaluated, the Artificial Neural Network (ANN) approach emerged as the most effective and reliable. Its superior efficiency, stability, and adaptability under both steady and dynamic irradiance conditions make it the recommended method for maximizing energy extraction and ensuring robust performance in photovoltaic systems.

While other algorithms like Incremental Conductance showed better performance than the commonly used Perturb and Observe method, they still fell short of the advanced capabilities offered by ANN-based MPPT. Consequently, for optimizing photovoltaic system output and ensuring long-term, reliable operation, the ANN algorithm stands out as the optimal solution among the methods studied

References

[1] B. Nour-Eddine, "Amélioration des performances de contrôle d'un système photovoltaïque par les méthodes métaheuristques," El Oued, Université Echahid Hamma Lakhdar. Faculté des Sciences et Technologie, 2013.

[2] S. Y. BOUDERHEM BRAHIM "Conception et Réalisation d'un Hacheur Boost MPPT à Base d'une Carte ARDUINO Application PV," 2017.

[3] S. Dwari and L. Parsa, "An efficient high-step-up interleaved DC–DC converter with a common active clamp," *IEEE Transactions on Power Electronics*, vol. 26, no. 1, pp. 66-78, 2010.

[4] F. L. Luo and H. Ye, *Advanced dc/dc converters*. crc Press, 2016.

[5] A. S. Y. Alzahrani, *Advanced topologies of high-voltage-gain DC-DC boost converters for renewable energy applications*. Missouri University of Science and Technology, 2018.

[6] R. P. Severns, G. Bloom, and R. P. Severns, *Modern DC-to-DC switchmode power converter circuits*. Springer, 1985.

[7] S. Chakraborty, H.-N. Vu, M. M. Hasan, D.-D. Tran, M. E. Baghdadi, and O. Hegazy, "DC-DC converter topologies for electric vehicles, plug-in hybrid electric vehicles and fast charging stations: State of the art and future trends," *Energies*, vol. 12, no. 8, p. 1569, 2019.

[8] https://www.toolify.ai/ai-news/complete-tutorial-implementing-ann-in-matlabsimulink-1764419#google_vignette (accessed.

[9] M. D. S. M. C. Mr MEKKAOUI Saddam and AhmedYahia, "(Conception, simulation et réalisation d'un régulateur solaire avec commande MPPT à base d'une carte Arduino) ", UNIVERSITE EchahidHamma Lakhdar- EL Oued, 2022.

[10] M. K. B. Abdelheq, "ETUDE ET REALISATION D'UN CONVERTISSEUR DC-DC," Université Aboubakr BelkaÔd-Tlemcen, 2018.

[11] S. ABBOUDA, "« Contribution à la commande des systèmes photovoltaïques »," Université de Reims Champagne-Ardenne et université de Sfax, 2015.

[12] R. Touahir and M. B. Zahia, "contrôleur neuronal pour la poursuite du point de puissance maximale d'un système photovoltaïque," *Mémoire master, Université Kasdi Merbah, Ouargla, Algérie,* 2015.

[13] S. H. E. Babaa, "High efficient interleaved boost converter with novel switch adaptive control in photovoltaic application," Newcastle University, 2013.

[14] A. b. T. Bekhti Mohammed, "Maximum Power Point Tracking Simulations for PV Applications Using Matlab Simulink," *International Journal of Engineering Practical Research,* January 2014.

[15] A. C. Pastor, "Conception et réalisation de modules photovoltaïques électroniques," INSA de Toulouse, 2006.

[16] M. R. Patel, *Wind and solar power system*. CRC press, 1999.

[17] R. Boukenoui, M. Ghanes, J.-P. Barbot, R. Bradai, A. Mellit, and H. Salhi, "Experimental assessment of Maximum Power Point Tracking methods for photovoltaic systems," *Energy,* vol. 132, pp. 324-340, 2017.

[18] B. N. Alajmi, K. H. Ahmed, S. J. Finney, and B. W. Williams, "Fuzzy-logic-control approach of a modified hill-climbing method for maximum power point in microgrid standalone photovoltaic system," *IEEE transactions on power electronics,* vol. 26, no. 4, pp. 1022-1030, 2010.

[19] A. A. Ghassami, S. M. Sadeghzadeh, and A. Soleimani, "A high performance maximum power point tracker for PV systems," *International Journal of Electrical Power & Energy Systems,* vol. 53, pp. 237-243, 2013.

[20] G. Abdelmounaim, "An Advanced Neural Network-Based MPPT Controller for Photovoltaic Systems," University of El-Oued, 2023.

[21] https://www.toolify.ai/ai-news/complete-tutorial-implementing-ann-in-matlabsimulink-1764419#google_vignette. (accessed.

[22] https://www.mathworks.com/help/deeplearning/ug/workflow-for-neural-network-design.html. (accessed.

Annex

Simulation used in ANN algorithm: